Article

Cell Reports

SFRPs Are Biphasic Modulators of Wnt-Signaling-Elicited Cancer Stem Cell Properties beyond Extracellular Control

Graphical Abstract

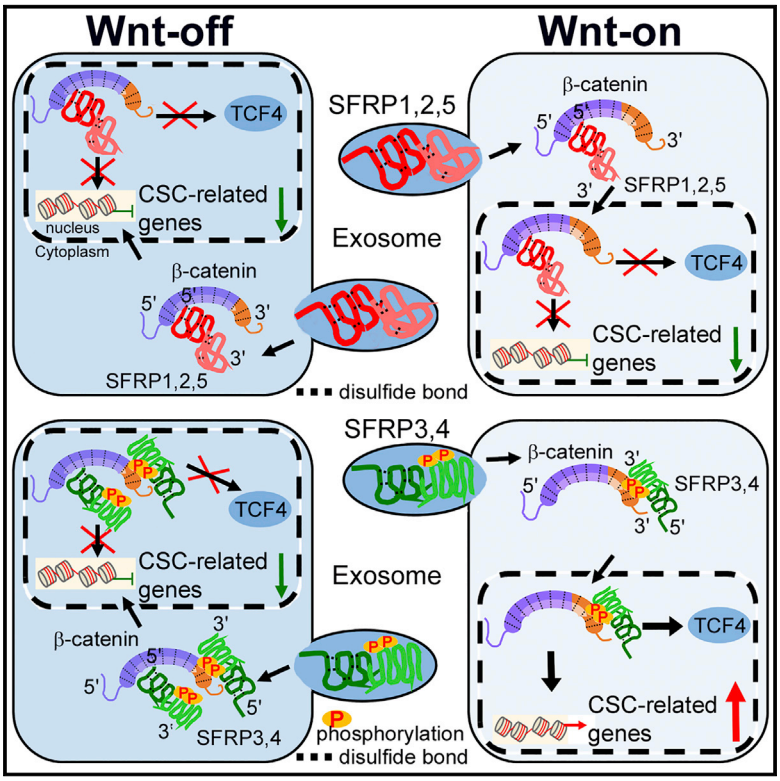

Highlights

- Aberrant, nuclear-localized SFRPs bind with β-catenin to modulate TCF4 recruitment
- The CRD and NTR domains of SFRPs have opposing regulatory effects on Wnt signaling
- SFRPs are biphasic modulators of Wnt signaling beyond extracellular control
- Tumor growth can be regulated by CRISPR/Cas9 for modulation of SFRPs expression

Authors

Chi-Jung Liang, Zih-Wun Wang, Yi-Wen Chang, Ko-Chuan Lee, Wei-Hsin Lin, Jia-Lin Lee

Correspondence

jllee@life.nthu.edu.tw

In Brief

Liang et al. find that CRD and NTR domains of nuclear SFRPs induce opposite effects on Wnt signaling by interacting with distinct β-catenin regions to modulate TCF4 recruitment. Disulfide bonds of CRD domain and two threonine phosphorylation events of NTR domain in SFRPs are required to generate Wnt/β-catenin-elicited CSC properties.

Liang et al., 2019, Cell Reports *28*, 1511–1525
August 6, 2019
https://doi.org/10.1016/j.celrep.2019.07.023

CellPress

Cell Reports
Article

SFRPs Are Biphasic Modulators of Wnt-Signaling-Elicited Cancer Stem Cell Properties beyond Extracellular Control

Chi-Jung Liang,[1] Zih-Wun Wang,[1] Yi-Wen Chang,[1] Ko-Chuan Lee,[1] Wei-Hsin Lin,[1,2] and Jia-Lin Lee[1,3,4,*]
[1]Institute of Molecular and Cellular Biology, National Tsing Hua University, Hsinchu 30013, Taiwan
[2]Department of Orthopedics, National Taiwan University Hospital Hsin-Chu Branch, Hsinchu 30059, Taiwan
[3]Department of Medical Science, National Tsing Hua University, Hsinchu 30013, Taiwan
[4]Lead Contact
*Correspondence: jllee@life.nthu.edu.tw
https://doi.org/10.1016/j.celrep.2019.07.023

SUMMARY

Secreted frizzled-related proteins (SFRPs) are mainly known for their role as extracellular modulators and tumor suppressors that downregulate Wnt signaling. Using the established (CRISPR/Cas9 targeting promoters of SFRPs and targeting SFRPs transcript) system, we find that nuclear SFRPs interact with β-catenin and either promote or suppress TCF4 recruitment. SFRPs bind with β-catenin on both their N and C termini, which the repressive effects caused by SFRP-β-catenin-N-terminus binding overpower the promoting effects of their binding at the C terminus. By high Wnt activity, β-catenin and SFRPs only bind with their C termini, which results in the upregulation of β-catenin transcriptional activity and cancer stem cell (CSC)-related genes. Furthermore, we identify disulfide bonds of the cysteine-rich domain (CRD) and two threonine phosphorylation events of the netrin-related motif (NTR) domain of SFRPs that are essential for their role as biphasic modulators, suggesting that SFRPs are biphasic modulators of Wnt signaling-elicited CSC properties beyond extracellular control.

INTRODUCTION

Previous studies have emphasized the importance of Wnt signaling in cancer cells. The Wnt/β-catenin signaling cascade serves as a critical regulator of normal stem cells as well as cancer stem cells (CSCs) (Chang et al., 2015; Reya and Clevers, 2005; Su et al., 2015a). A recent study demonstrated that Wnt signaling may be responsible for enhancing the self-renewal capacity and stem cell characteristics of prostate cancer cells (Bisson and Prowse, 2009).

The secreted frizzled-related protein (SFRP) family is composed of five secreted glycoproteins, namely, SFRP1, SFRP2, SFRP3 (Frzb), SFRP4, and SFRP5, which have been identified in humans, mice, and chickens (Leimeister et al., 1998; Terry et al., 2000). SFRPs contain a cysteine-rich domain (CRD) that is 30% to 50% similar in sequence homology with the CRD of the Frizzled protein at the N terminus and with a netrin-related motif (NTR) at the C terminus. SFRPs have been known to modulate the Wnt signaling pathway by directly binding with Wnt ligands to block the interaction between the Wnt and Frizzled receptor. SFRPs can also bind with the Frizzled receptor to form a non-functional complex that prevents Wnt signaling activation (Bafico et al., 1999). Although SFRPs are important Wnt signaling regulators, it remains uncertain whether SFRPs modulate the Wnt signaling pathway only extracellularly or by other mechanisms.

Among the five members of the SFRP family, SFRP1 has been more thoroughly studied. SFRP1 has a biphasic effect on Wnt signaling. At low concentrations, SFRP1 increases Wnt activity; however, Wnt activity is reduced under high concentrations of SFRP1 (Uren et al., 2000). Other SFRP promoters have also been found to undergo epigenetic modification in different types of cancers, including SFRP2 in gastric cancer, SFRP3 in hepatocellular carcinoma, SFRP4 in mesothelioma, and SFRP5 in breast cancer (Cheng et al., 2007; He et al., 2005; Lin et al., 2014; Veeck et al., 2008). Although mutations in SFRP genes thus far have not been directly linked to diseases, SFRPs have been considered tumor suppressor genes. Nevertheless, recent research suggests that SFRPs may have different regulatory roles in the Wnt signaling pathway and cause distinct effects in different types of cancer.

However, many questions regarding the SFRP family remain: (1) do different SFRP family members have opposing effects on the same process; (2) are certain actions of SFRPs that are independent of the SFRP-Wnt interaction also required to endogenously modulate Wnt signaling; and (3) do post-translational modifications create additional differences that might further diversify the functions of the different SFRP family members?

Most SFRP functions that have been discussed thus far relate to their effect on Wnt signaling through a direct interaction with Wnt. However, determining the SFRP binding domains and their affinities alone is insufficient to understand how SFRPs antagonize Wnt signaling in living cells because biochemically demonstrated Wnt-SFRP interactions are not necessarily functional *in vivo* (Lin et al., 1997; Wawrzak et al., 2007). It is possible that additional molecules are required to regulate SFRP-Wnt activities in living cells. Thus, further studies are needed to clarify

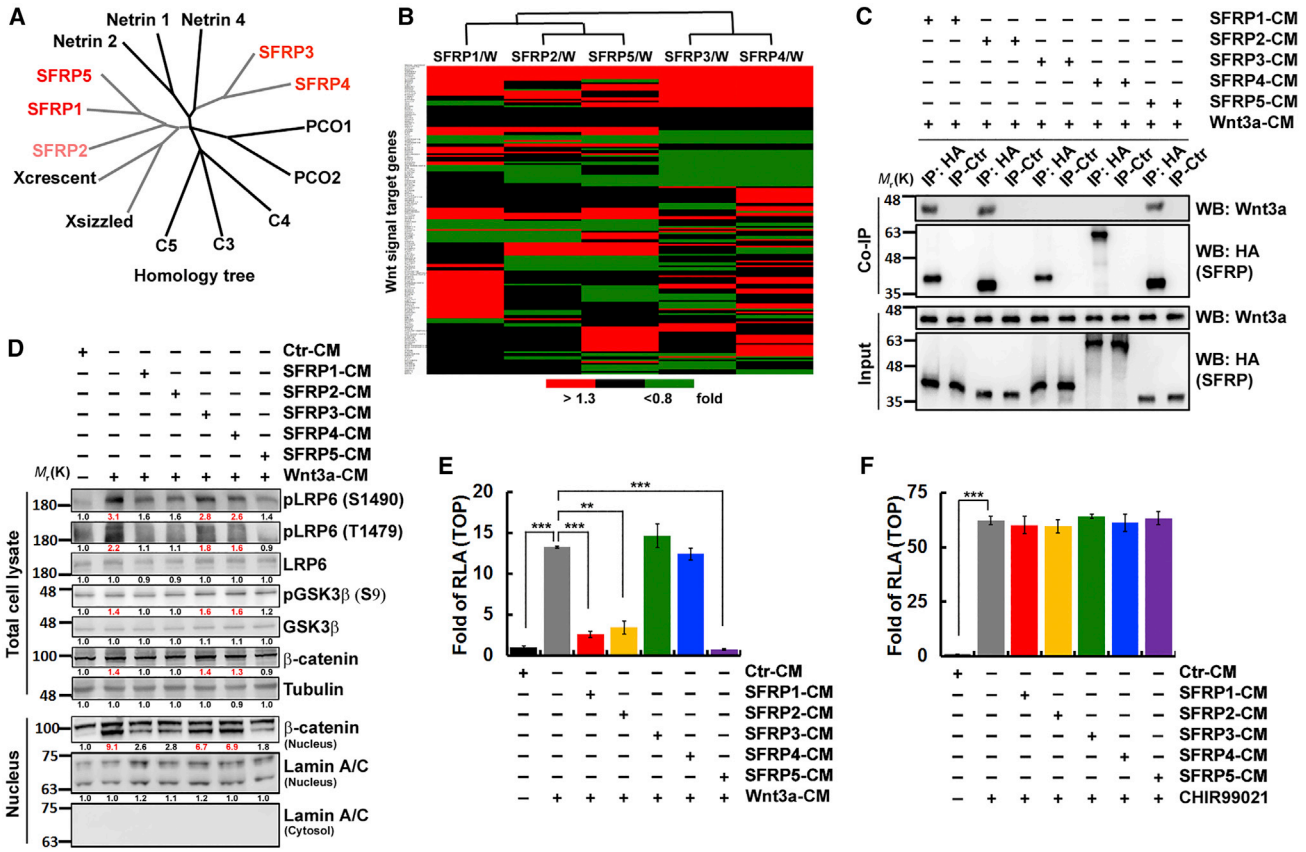

Figure 1. SFRP1, SFRP2, and SFRP5 Appear Most Closely Related, whereas SFRP3 and SFRP4 Form a Separate Subgroup

(A) Phylogenetic analysis of SFRPs.

(B) Microarray analysis was performed on the expression profiles of SFRP-expressing stable clones after treatment with Wnt3a (W)-containing medium. Representative clusters of the indicated genes are shown as heatmaps, with red indicating increased expression and green indicating decreased expression, as indicated by the color intensity scale shown below each heatmap.

(C) The conditional medium was prepared from mock, SFRP-HA-, or Wnt3a-expressing stable clones. SFRP-CM was mixed with Wnt3a-CM and incubated at 37°C for 1 h. After concentration, the mixed media were immunoprecipitated using anti-HA followed by western blotting.

(D) Western blotting analysis of the total cell lysates and nuclear fractions prepared from HM20 cells after treatment with the mixed media, as described in (C).

(E) Total cell lysates were prepared from HM20 cells, as described in (D). A TOPflash luciferase reporter assay was performed.

(F) Total cell lysates were prepared from HM20 cells after treatment with SFRP-CM containing 3 μM CHIR99021 for 6 h. A TOPflash luciferase reporter assay was performed.

Data in (E) and (F) were derived from three independent experiments and are presented as the mean ± SEM. *$p < 0.05$; **$p < 0.01$; ***$p < 0.005$ (t test). Ctr, control; CM, conditional medium; RLA, relative luciferase activity.

how SFRP activity is integrated into cellular signaling pathways and to identify other role of SFRPs, either in a Wnt-dependent or Wnt-independent manner.

In this study, abnormal nuclear localization of SFRPs bound to β-catenin was found to modulate TCF4 recruitment, which, as a result, exerted either promoting or suppressive effects on the Wnt/β-catenin-elicited CSC phenotype. The CRD and NTR domains of SFRPs were shown to induce opposite regulatory effects as those demonstrated in earlier research on Wnt signaling by interacting with distinct β-catenin regions. Disulfide bonds of the CRD domain and two threonine phosphorylation events of the NTR domain in SFRPs were required to generate Wnt/β-catenin-elicited CSC properties. Taken together, our results identify SFRPs as biphasic modulators of Wnt-signaling-elicited CSC properties beyond extracellular control.

RESULTS

SFPR1, SFRP2, and SFRP5 Appear Most Closely Related, whereas SFRP3 and SFRP4 Form a Separate Subgroup

To start, we investigated the relationship between the SFRPs. The sequence comparison and phylogenetic analysis indicated that SFRP1, SFRP2, and SFRP5 are closely related, whereas SFRP3 and SFRP4 are more similar to one another and belong to a different subgroup to that of the other three SFRP proteins (Figure 1A). To further support this observation, we treated stable clones expressing the different SFRPs with Wnt3a-containing medium (Wnt3a-CM). Microarray analysis also demonstrated that SFRP1, SFRP2, and SFRP5 had a similar expression profile and that SFRP3 and SFRP4 are closely related

(Figure 1B). Moreover, the SFRPs in the same subgroup showed similar interactions with other proteins. We incubated conditional media collected from SFRPs-hemagglutinin (HA)- and Wnt3a-expressing stable clones (SFRPs-CM and Wnt3a-CM, respectively), and we observed that SFRP1, SFRP2, and SFRP5 bound to Wnt3a extracellularly, whereas SFRP3 and SFRP4 did not (Figure 1C). We also found that extracellular SFRP1, SFRP2, and SFRP5 secreted from cells could have a greater repressive impact on signaling induced by Wnt3a, whereas SFRP3 and SFRP4 did not (Figure 1D). These results were identified using TOPflash luciferase reporter assays (Figure 1E). However, once β-catenin transcriptional activity was directly activated with the GSK-3β inhibitor (CHIR99021) treatment (activating the Wnt signaling pathway by bypassing extracellular control), all SFRPs, regardless of the subgroup they belonged to, lost the ability to repress Wnt3a signals in an extracellular setting (Figure 1F). Secreted SFRPs were also unable to inhibit the transcriptional activity of β-catenin in GSK-3β inhibitor-treated cells, suggesting that the ability of extracellular SFRPs to inhibit Wnt signaling is Wnt3a-ligand-dependent.

SFRPs Are Biphasic Modulators of Wnt Signaling beyond Extracellular Control

After establishing the properties and functions of each SFRP in the extracellular setting, we investigated whether SFRPs would exert control over cellular functions intracellularly. All extracellular SFRPs translocated into the nucleus upon long-term (72 h) SFRP-CM treatment (Figure 2A). Consistent with the results shown in Figure 2A, SFRP nuclear translocation was also observed in SFRP-expressing modified cells by CRISPR/Cas9 technology (SFRP-knockout [KO]: a single guide RNA [sgRNA] was designed to target human *SFRP1*, and SFRP1-KO was performed by CRISPR/Cas9 technology; SFRP2-5-ACT: sgRNAs were designed to target the SFRP2-5 promoters, and dCas9-P300 was chosen for their enhanced chromatin-remodeling activity) (Figure 2B); we used these cell lines in future experiments. In these SFRP-expressing modified cells, SFRP1, SFRP2, and SFRP5 greatly repressed Wnt3a-induced transcriptional activity upon Wnt3a-CM treatment. By contrast, SFRP3 and SFRP4 significantly promoted Wnt3a-induced transcriptional activity (Figure 2C). The repressive effects of SFRP1, SFRP2, and SFRP5 decreased with 3 μM CHIR99021 treatment, but the overall pattern was consistent with that following Wnt3a-CM treatment (Figure 2D). Next, we sought to determine whether different concentrations of CHIR99021 altered SFRP activity. Regardless of the CHIR99021 concentration, the suppressive effects of SFRP1, SFRP2, and SFRP5 remained constant. Interestingly, SFRP3 reversed its repressive role to a promoting role at CHIR99021 concentrations of more than 3 μM. This phenomenon was observed for SFRP4 only at CHIR99021 concentrations of more than 5 μM (Figure 2E). In SFRP-expressing modified cells with high levels of SFRP expression, all SFRPs repressed the CHIR99021-induced transcriptional activity. SFRP1, SFRP2, and SFRP5 remained as suppressors, and SFRP3 and SFRP4 functioned as enhancers to CHIR99021-induced transcriptional activity in cells expressing low levels of SFRP (Figure 2F).

According to our recent research (Chang et al., 2015), we documented that Twist1 binding to β-catenin enhanced the transcriptional activity of the β-catenin/TCF4 complex, including by binding to the proximal promoter region of CSC-related genes. In agreement with this notion, the promoting effects of SFRP3 and SFRP4 became more significant when the cells expressed increased levels of Twist1 (Figure 2G).

Aberrant, Nuclear-Localized SFRPs Bind with β-Catenin to Modulate TCF4 Recruitment

We next used immunohistochemistry to observe SFRP localization in human lung cancer. According to the clinical samples collected from tissue slices of patients with lung cancer, all SFRPs were expressed in the nucleus (Figure 3A). The SFRPs of several lung cancer cell lines were also seen to translocate into the nucleus (Figure 3B). Recent studies have identified several factors that are required for the secretion of SFRP proteins; however, how SFRPs travel in the extracellular space remains a largely unresolved question. Here, we show that SFRPs were secreted by exosomes, which can be decreased by transfection with a small interfering RNA (siRNA) targeting *YKT6* (Figure 3C). We further tested if HM20 cells could naturally take up SFRP-containing exosomes. HM20 cells were incubated with the isolated exosomes derived from SFRP-expressing modified cells for the time points indicated, and exosome uptake was determined by western blotting. Extracellular SFRPs can naturally be taken up by cells by SFRP-containing exosomes and can translocate into the nucleus (Figure 3D). To further dissect the molecular mechanisms of SFRP-elicited signaling, we used stable clones expressing the different SFRP-HA in future experiments. The nuclear fraction of the stable clones indicated that all SFRPs could bind to β-catenin (Figure 3E). Moreover, immunofluorescence data demonstrated that SFRP1–5 co-localized with β-catenin in both the cytoplasm and nucleus (Figure 3F). The nuclear translocation of SFRPs can be abolished after knock down of β-catenin, indicating the nuclear translocation of SFRPs was β-catenin-dependent (Figure 3G). By co-immunoprecipitation (coIP), we determined that SFRP1, SFRP2, SFRP4, and SFRP5 suppressed TCF4 binding to β-catenin after treatment with Wnt3a-CM; conversely, SFRP3 promoted this binding (Figure 3H).

The CRD and NTR Domains of SFRPs Have Opposing Regulatory Effects on Wnt Signaling through Their Association with Distinct Regions of β-Catenin

CoIP experiments revealed that SFRPs and TCF4 were in complex with β-catenin after treatment with Wnt3a-CM (Figure 3H). In-frame β-catenin and SFRP deletion mutants were generated for mapping the interacting domains in SFRPs and β-catenin (Figures 4A and 4C). CoIP analysis showed that the N terminus of β-catenin was important for this interaction with all SFRPs, whereas the C terminus of β-catenin could bind SFRP3 and SFRP4 only (Figure 4B). Furthermore, all SFRPs could bind with the N terminus β-catenin at their N termini (Figure 4D), which repressed β-catenin transcriptional activity (Figure 4G). Only SFRP3 and SFRP4 could bind to the C terminus of β-catenin with their C termini (Figure 4D), and this conversely promoted β-catenin transcriptional activity (Figure 4G). By coIP,

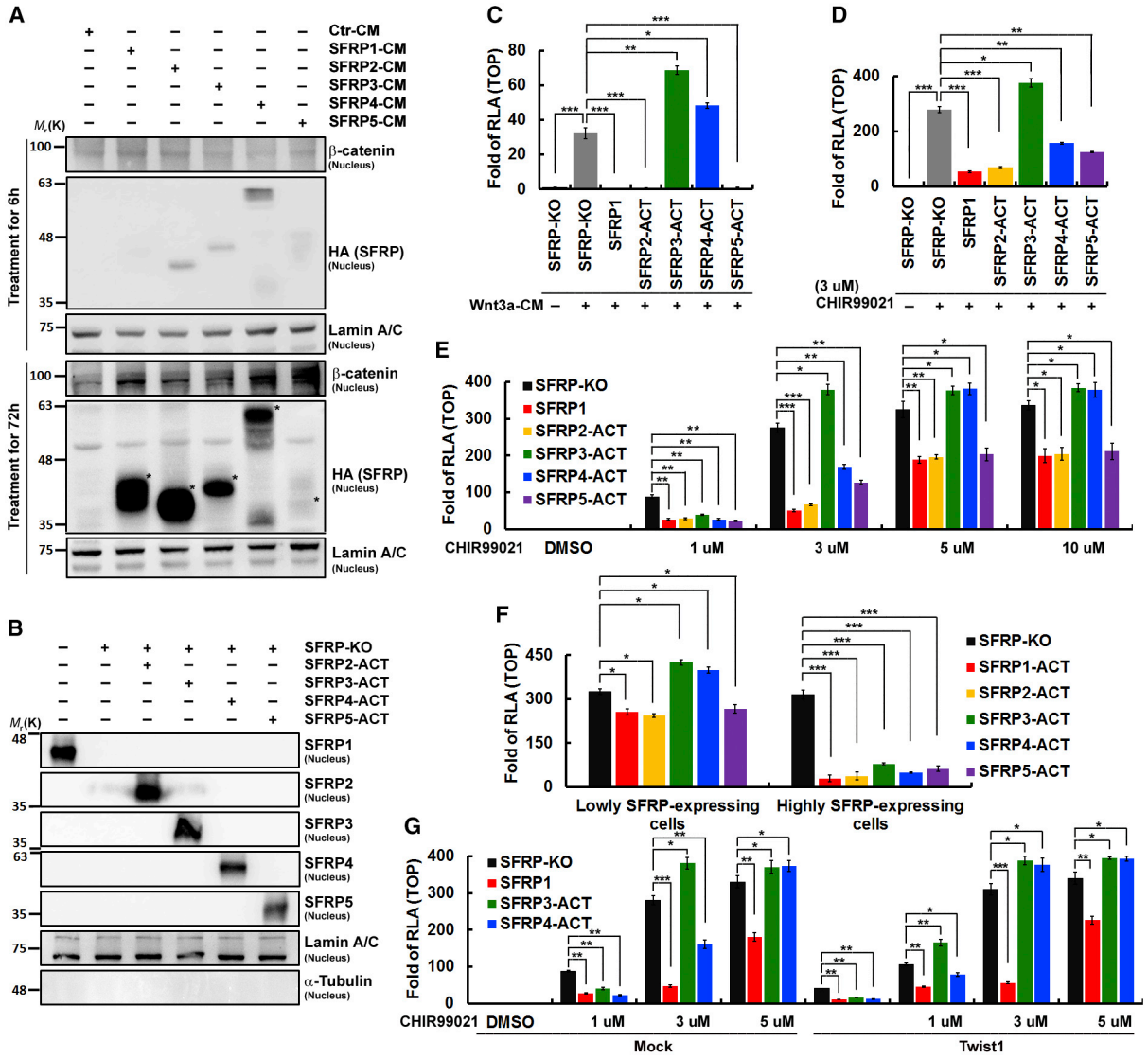

Figure 2. SFRPs Are Biphasic Modulators of Wnt Signaling beyond Extracellular Control

(A) Western blotting analysis of nuclear fractions prepared from HM20 cells after treatment with Ctr-CM or SFRP-CM for 6 h (top panel) or 72 h (bottom panel).

(B) Western blotting analysis of nuclear fractions prepared from SFRPs-expressing modified cells by CRISPR/Cas9 technology. SFRP-KO: a single guide RNA (sgRNA) was designed to target human *SFRP1*, and SFRP1 knock out was performed by CRISPR/Cas9 technology; SFRP2-5-ACT: sgRNAs were designed to target the SFRP2–5 promoters, and dCas9-P300 was chosen for their enhanced chromatin-remodeling activity.

(C–D) Total cell lysates were prepared from SFRPs-expressing modified cells by CRISPR/Cas9 technology as described in (B) after treatment with Wnt3a-CM (C) or 3 μM CHIR99021 (D) for 24 h. TOPflash luciferase reporter assays were performed.

(E) Total cell lysates were prepared from SFRPs-expressing modified cells by CRISPR/Cas9 technology as described in (B) after treatment with increasing concentrations (1, 3, 5, and 10 μM) of CHIR99021 for 24 h. TOPflash luciferase reporter assays were performed.

(F) Total cell lysates were prepared from low- and high-SFRPs-expressing cells (derived from SFRPs-expressing modified cells by CRISPR/Cas9 technology as described in B) after treatment with 3 μM CHIR99021 for 24 h. TOPflash luciferase reporter assays were performed.

(G) Total cell lysates were prepared from SFRPs-expressing modified cells by CRISPR/Cas9 technology as described in (B) transfected with plasmids encoding Twist1 after treatment with increasing concentrations (1, 3, and 5 μM) of CHIR99021 for 24 h. TOPflash luciferase reporter assays were performed.

Data in (C)–(G) are derived from three independent experiments and are presented as the mean ± SEM. *$p < 0.05$; **$p < 0.01$; ***$p < 0.005$ (t test). Ctr, control; CM, conditional medium; TOP, TOPflash luciferase reporter assay; RLA, relative luciferase activity.

we determined that SFRP1 suppressed TCF4 binding to β-catenin after treatment with Wnt3a-CM; conversely, SFRP3 promoted this binding (Figure 3I). According to previous research, disulfide bonds are essential for the formation and stability of SFRPs (Chong et al., 2002). In our study, we further found that the loss of cysteine (four cysteines [C58/68/129/133] of SFRP1 were substituted with alanine; SFRP1^{4CA}) resulted in SFRP1 loss of association with β-catenin and loss of ability to inhibit

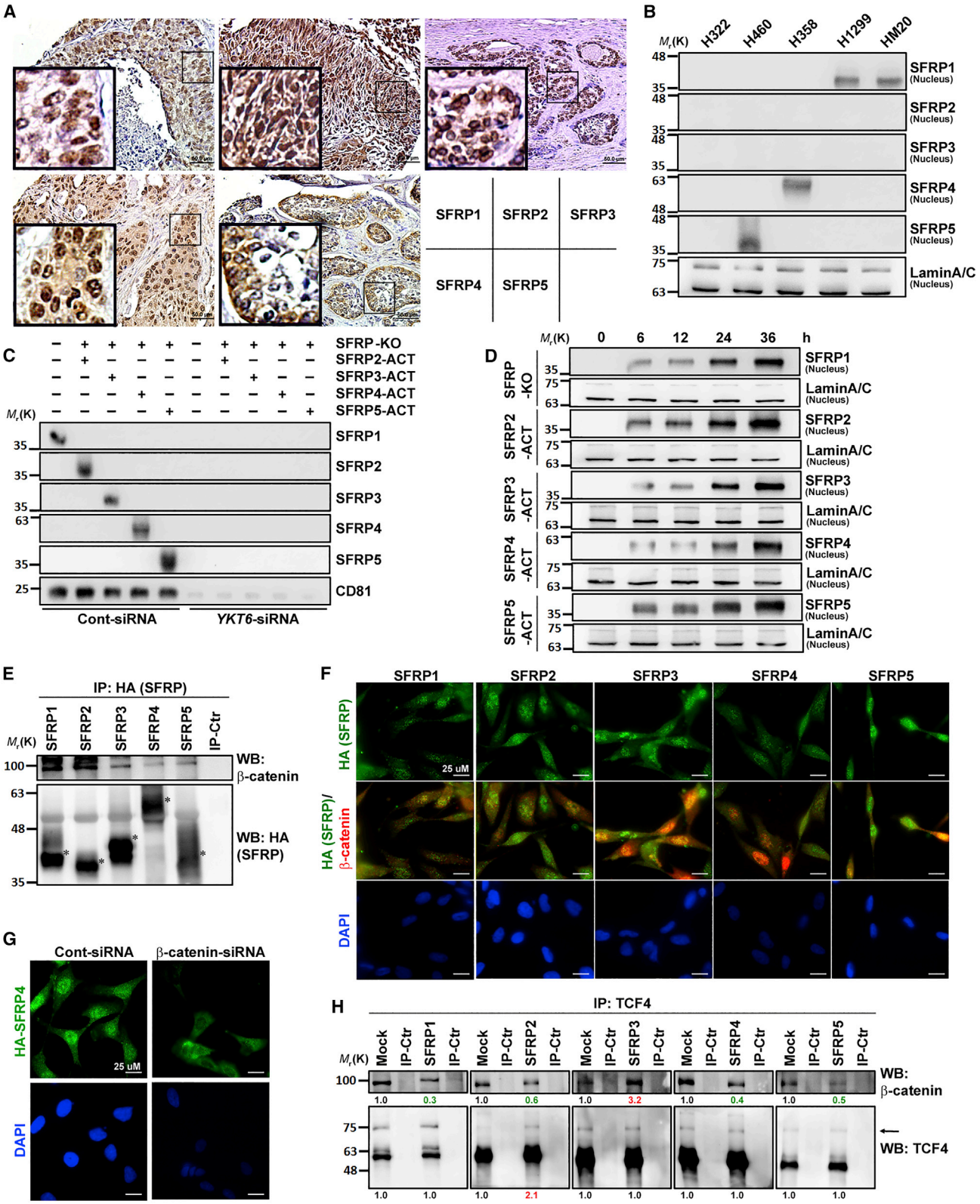

(legend on next page)

TCF4 and Twist1 recruitment (Figure 4E). Our results also demonstrated the importance of threonine186/189 phosphorylation for the C terminus function of SFRP4. Consistent with the results shown in Figure 4D, SFRP4 could bind with both the N and C termini on β-catenin. SFRP4^{2TA} (two threonine [T186/189] of SFRP4 were replaced with alanine) could not disrupt the association with β-catenin (Figure 4F). However, SFRP4^{2TA} resulted in a loss of the ability to enhance TCF4 and Twist1 recruitment (Figure 4F), and further eliminated their biological functions in enhancing β-catenin transcriptional activity (Figure 4G). Further analysis was complicated by the fact that there are high- and low-affinity binding sites on the SFRPs for β-catenin and that the binding affinities between various SFRP-β-catenin pairs might differ. Regardless of the expression level of β-catenin and SFRP1, SFRP1 could only bind with the N terminus of β-catenin, and the disulfide-bond-formation-deficient mutant (SFRP1^{4CA}) disrupted this association (Figure 4H). For cells that have β-catenin^{High}/SFRP4^{Low} in the nucleus (low expression), β-catenin and SFRP4 could only bind with their C termini, indicating a stronger binding affinity between the C termini of SFRP4 and β-catenin (Figure 4I), which resulted in the upregulation of β-catenin transcriptional activity (Figure 4G). When β-catenin^{Low}/SFRP4^{High} was present in the nucleus, SFRP4 could bind with β-catenin on both of its N and C termini (Figure 4I). However, the repressive effects caused by SFRP-β-catenin-N-terminus binding overpowered the promoting effects of the proteins that bound at the C terminus (Figure 4G).

Nuclear SFRPs Are Potent Modulators of Wnt/β-Catenin-Elicited Promotion of the CSC Phenotype

Cancer cells with the CSC phenotype show increased sphere-forming ability. Here, we demonstrated that SFRP-expressing modified H358 cells by CRISPR/Cas9 technology upon 5 μM CHIR99021 treatment and SFRP1-, 2-, and SFRP5-expressing cells showed poor sphere-forming ability, whereas SFRP3 and SFRP4 promoted sphere formation (Figure 5A). These results remained consistent in SFRP-expressing modified H1299 (Figure 5B) and HM20 (Figure 5C) cells by CRISPR/Cas9 technology and stable clones expressing the different SFRP-HA in HM20 cells (Figure 5D). Stimulation with 5 μM CHIR9902 suppressed (SFRP1) and promoted (SFRP4) sphere formation (Figure 5E), as well as the expression of stem-cell-related and ABC transporter genes (Figure 5G), whereas an alanine-substituted mutation on both SFRPs (SFRP1^{4CA} and SFRP4^{2TA}) did not (Figures 5E and 5G). These results were confirmed by chromatin immunoprecipitation (ChIP) assays. After 5-μM CHIR99021 treatment, HA-SFRP4 bound to the proximal promoter regions of *PROM1* and *ABCG1* but HA-SFRP1 did not (Figure 5F). After 5 μM CHIR99021 treatment, β-catenin in wild-type SFRP4-expressing cells bound to the proximal promoter regions of *PROM1* and *ABCG1*, whereas β-catenin in cells expressing an alanine-substituted mutation on SFRP4 (SFRP4^{2TA}) did not (Figure 5F). Conversely, β-catenin in wild-type SFRP1-expressing cells did not bind to the proximal promoter regions of *PROM1* and *ABCG1* after 5 μM CHIR99021 treatment, whereas β-catenin in cells expressing an alanine-substituted mutation on SFRP1 (SFRP1^{4CA}) did (Figure 5F). Furthermore, CSCs are capable of excluding the fluorescent dye Hoechst 33342. Hence, the isolated cells in the side population represented cancer cells with the CSC phenotype. Following 5 μM CHIR99021 treatment, we observed that SFRP1 suppressed the side population, whereas SFRP4 promoted these cells (Figure 5H). An alanine-substituted mutation on both SFRPs (SFRP1^{4CA} and SFRP4^{2TA}) eliminated the biological functions of these proteins (Figure 5H).

Clinical Significance of Nuclear SFRPs, Twist1, and CD133 in Human Patients with Lung Cancer

To further validate our results, we used immunohistochemistry staining and scoring of tumor tissues collected from human lung cancer patients. CD133 lacked the apparent decrease of expression in tumor cells that expressed high levels of cytosolic SFRP1, 2, and 5. However, high levels of expression of nuclear SFRP1, 2, and 5 were accompanied by a significant reduction of CD133 expression (Figure 6A). Spearman's rank test also indicated the inverse relationship between nuclear SFRP1, 2, and 5 and CD133 expression. By contrast, cytosolic SFRP3 demonstrated a positive correlation with CD133 expression, and this relationship was more significant between nuclear SFRP3 and CD133 expression (Figure 6B). High Twist1 expression further strengthened this correlation. CD133 expression was high when both nuclear SFRP3 and Twist1 expression

Figure 3. Aberrant, Nuclear-Localized SFRPs Bind with β-Catenin to Modulate TCF4 Recruitment

(A) Immunohistochemistry of nuclear SFRPs in human lung cancer specimens by using anti-SFRP1–5 antibodies with nuclei counterstained with hematoxylin. Left bottom, enlarged images from boxed areas as indicated. Bars, 50 μm.

(B) Western blotting analysis of nuclear fractions prepared from human lung cancer cell lines.

(C) Exosomes were isolated from CM derived from cells (SFRP-expressing modified cells by CRISPR/Cas9 technology as described in Figure 2B) transfected with a siRNA targeting *YKT6*, and protein lysates were used to perform western blotting for CD81 (an exosome marker).

(D) HM20 cells were incubated with the isolated exosomes derived from SFRP-expressing modified cells by CRISPR/Cas9 technology as described in Figure 2B for the time points indicated, and exosome uptake was determined by western blotting.

(E) Nuclear fractions were prepared from SFRP-HA-expressing stable clones and then immunoprecipitated using anti-HA followed by western blotting.

(F) Immunostaining for SFRPs (HA-tag; green) and μ-catenin (red) is shown in HM20 cells incubated with the isolated exosomes derived from HA-SFRPs-expressing cells for 48 h prior to Wnt3a-CM treatment for 4 h. Nuclei were counterstained with 4′,6-diamidino-2-phenylindole (DAPI; blue). Bars, 25 μm.

(G) HM20 cells were transfected with siRNA targeting μ-catenin prior to the isolated exosomes (derived from HA-SFRP4-expressing cells) incubation followed by immunostaining. Immunostaining for SFRP4 (HA-tag; green) is shown. Nuclei were counterstained with DAPI (blue; lower panels). Bars, 25 μm.

(H) Nuclear fractions were prepared from SFRP-HA-expressing stable clones after treatment with Wnt3a-CM (the expression level of SFRPs and related proteins was determined by western blotting and shown in Figure S1) and then immunoprecipitated using anti-TCF4 followed by western blotting. The relative intensities of the bands are shown.

Ctr, control; CM, conditional medium.

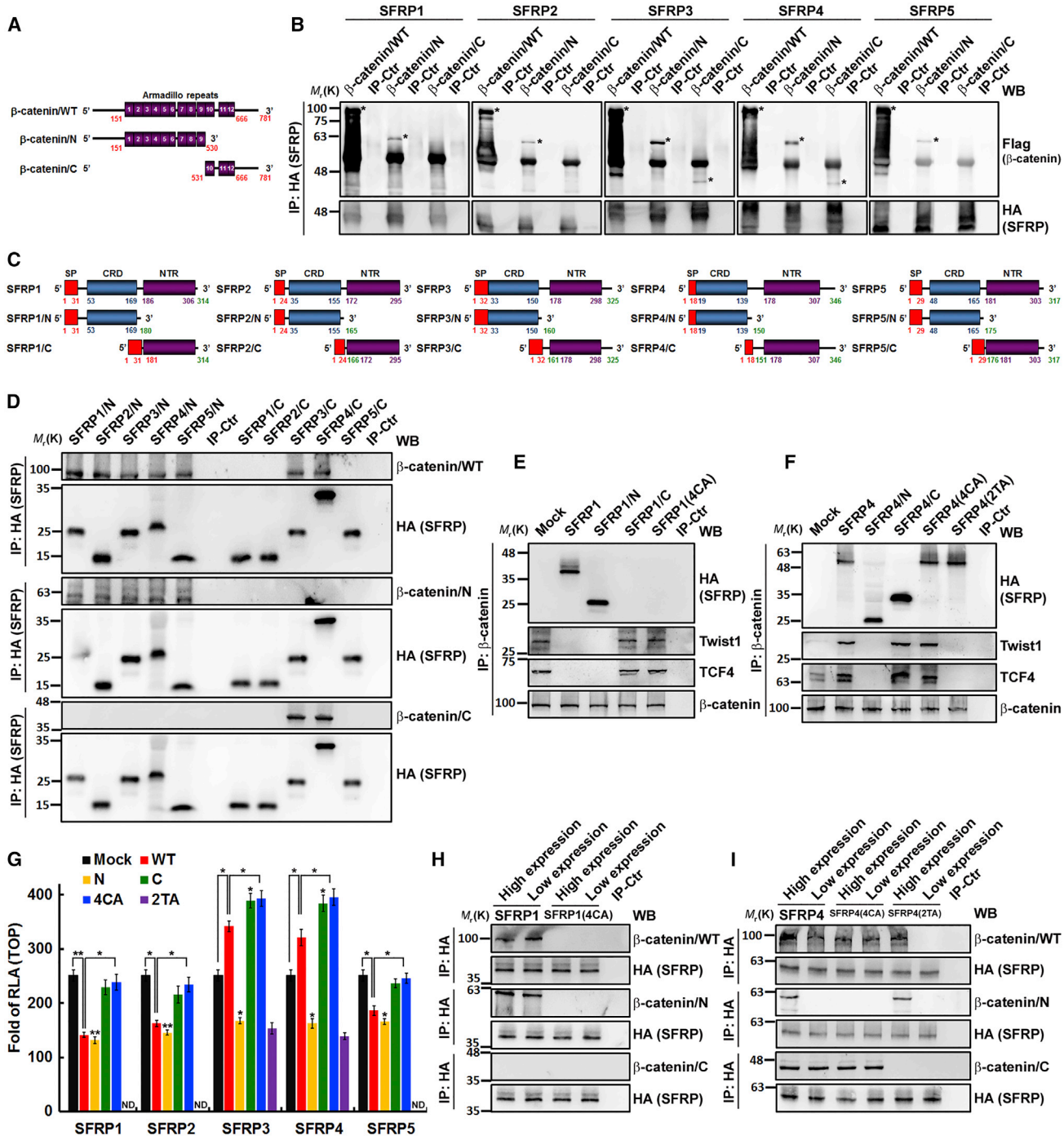

Figure 4. The CRD and NTR Domains of SFRPs Have Opposing Regulatory Effects on Wnt Signaling through Their Association with Distinct Regions of β-Catenin

(A) Schematic representation of FLAG-tagged wild-type (β-catenin/WT), the N terminus (β-catenin/N), and C terminus (β-catenin/C) β-catenin proteins.

(B) SFRP-HA-expressing stable clones were transfected with FLAG-tagged wild-type β-catenin and deletion mutants as described in (A). Nuclear fractions were prepared from cells (the expression level of SFRP-HA and FLAG-β-catenin was determined by western blotting and shown in Figure S2) and then immunoprecipitated using anti-HA followed by western blotting. Asterisks, truncated forms of β-catenin proteins at expected sizes.

(C) Schematic representation of HA-tagged wild-type (SFRPs), the N terminus (SFRPs/N), and C terminus (SFRPs/C) SFRP proteins. SP, signal peptide; CRD, cysteine-rich domain; NTR, netrin-related motif.

(legend continued on next page)

were also high, whereas low CD133 expression was associated with low nuclear SFRP3 expression (Figure 6C). We then quantified our findings by separating the samples into four categories based on the level of nuclear SFRP3 and Twist1 expression. High Twist1 expression led to increased CD133 expression, and the effect was further promoted with high nuclear SFRP3 expression (Figure 6D). This relationship between SFRP, Twist1, and CD133 was also observed for SFRP4 (Figures 6E and 6F).

Disulfide Bonds of the CRD Domain and Threonine$^{186/189}$ Phosphorylation of the NTR Domain in SFRPs Are Required for Modulating Wnt/β-Catenin-Elicited CSC Properties in Experimental Animal Models

Next, we sought to verify our results in animal models. We treated 10^2 SFRP-expressing cells with 5 μM CHIR99021 before injecting these cells subcutaneously into mice. Consistent with previous results, SFRP1, 2, and 5 repressed tumorigenic potential and tumor growth, whereas SFRP3 and 4 promoted these effects. The function of SFRPs was abolished with a mutation in the CRD (4CA) and a threonine of the NTR domain (2TA) (Figures 7A and 7B). To test whether cancer cells derived from xenografts exhibited the properties of CSCs, the resultant tumors were analyzed. The expression of the CSC marker CD133 was suppressed by SFRP1, 2, and 5, whereas the function of its mutant form (SFRP1^{4CA}) was lost. The unphosphorylatable mutant form of SFRP4 (SFRP4^{2TA}) also lost its original ability to promote CD133 expression (Figure 7C).

Based on our findings, we propose a model that explains the mechanism between nuclear SFRPs and the Wnt/β-catenin signaling pathway, as well as how their interaction regulates CSC-related genes. According to previous research, disulfide bonds are essential for the formation and stability of SFRPs because the loss of cysteine (SFRP1–5^{4CA}) results in the proteins' loss of function (Figures 7D and 7E). In addition, our results indicate a mechanism demonstrating the importance of two threonine phosphorylation events on the function of the SFRP3 and SFRP4 C terminus (Figure 7F). All SFRPs can bind to the N terminus of β-catenin with their N termini (CRD domains, SFRP1–5^{4CA} can disrupt the interaction), which represses β-catenin transcriptional activity and CSC-related genes. Only SFRP3 and SFRP4 bind to the C terminus of β-catenin with their C termini (NTR domains, SFRP3–4^{2TA} can disrupt the interaction), which conversely promotes β-catenin transcriptional activity and increases CSC-related gene expression. The binding affinity between the C termini of SFRPs and β-catenin is stronger. Therefore, when there is limited β-catenin or higher levels of SFRP3 and SFRP4 in the nucleus, SFRPs bind with β-catenin on both their N termini and C termini. However, the repressive effects caused by SFRP-β-catenin-N-terminus binding overpower the promoting effects of the proteins' binding at the C terminus. As a result, the overall β-catenin transcriptional activity and expression of CSC-related genes are downregulated (Figure 7F, left). On the contrary, for cells that have abundant β-catenin or low levels of SFRP3 and SFRP4 in the nucleus (by high Wnt activity), β-catenin and SFRPs only bind with their C termini, which results in the upregulation of β-catenin transcriptional activity and CSC-related genes (Figure 7F, right).

Tumor Growth Can Be Regulated by CRISPR/Cas9-Mediated Epigenome Editing for Precision Modulation of SFRP Expression *In Vitro* and in Experimental Animal Models

For *in vitro* tumor growth assays, dCas9-P300 stable clones (1,000/mL) with Wnt3a treatment were cultured under sphere-forming conditions. After 8 days, these spheres reached an approximate average volume (spheres with a diameter > 30 μm) and would be infected every other day for a period of 5 days with specific viral particles containing constructs encoding sgRNAs that were designed to target the SFRP1 and SFRP4 promoters. HM-dCas9-P300 cells transfected with viral particles containing constructs encoding sgRNAs targeting the SFRP4 promoters further enhanced the Wnt3a-elicited tumor growth, whereas HM-dCas9-P300 cells transfected with viral particles containing constructs encoding sgRNAs targeting the SFRP1 promoters significantly suppressed the Wnt3a-elicited tumor growth (Figure 7G). For *in vivo* tumorigenicity assays, mice were injected subcutaneously with 10^2 cells (dCas9-P300 stable clones). After 20 days, these tumors reached an approximate average volume and would be injected intratumorally every 4 days for a period of 13 days with specific viral particles containing constructs encoding sgRNAs that were designed to target the SFRP1 and SFRP4 promoters. Consistent with the results performed *in vitro*, intratumoral injections of virus particles containing constructs

(D) Stable clones expressing SFRP-HA (deletion mutants as described in C) were transfected with FLAG-tagged wild-type β-catenin and deletion mutants as described in (A). Nuclear fractions were prepared from cells (the expression level of SFRP-HA and FLAG-β-catenin was determined by western blotting and shown in Figure S3) and then immunoprecipitated using anti-HA followed by western blotting.

(E and F) Stable clones expressing SFRP-HA (wild type and mutants; SFRP1 in E; SFRP4 in F) were treated with 3 μM CHIR99021 for 24 h. Nuclear fractions were prepared from cells (the expression level of Wnt-related proteins was determined by western blotting and shown in Figures S4 and S5) and then immunoprecipitated using anti-β-catenin followed by western blotting.

(G) Total cell lysates were prepared from stable clones expressing SFRP-HA (wild type and mutants) after treatment with 5 μM CHIR99021 for 24 h. A TOPflash luciferase reporter assay was performed. Data were derived from three independent experiments and are presented as the mean ± SEM. *$p < 0.05$; **$p < 0.01$ (t test). ND, not determined; RLA, relative luciferase activity.

(H and I) High and low expression clones were selected from stable clones expressing SFRP-HA (wild type and mutants; SFRP1 in H; SFRP4 in I) followed by transfection with FLAG-tagged wild-type β-catenin and deletion mutants, as described in (A). Nuclear fractions were prepared from cells (the expression level of SFRP-HA and FLAG-β-catenin was determined by western blotting and shown in Figures S6 and S7) and then immunoprecipitated using anti-HA followed by western blotting.

SFRP1^{4CA}, SFRP1(C58/68/129/133A); SFRP2^{4CA}, SFRP2(C40/50/114/118A); SFRP3^{4CA}, SFRP3(C35/43/108/112A); SFRP4^{4CA}, SFRP4(C24/32/97/101A); SFRP5^{4CA}, SFRP5(C53/63/124/128A); SFRP3^{2TA}, SFRP3(T186/189A); SFRP4^{2TA}, SFRP4(T186/189A); Ctr, control; WB, western blotting.

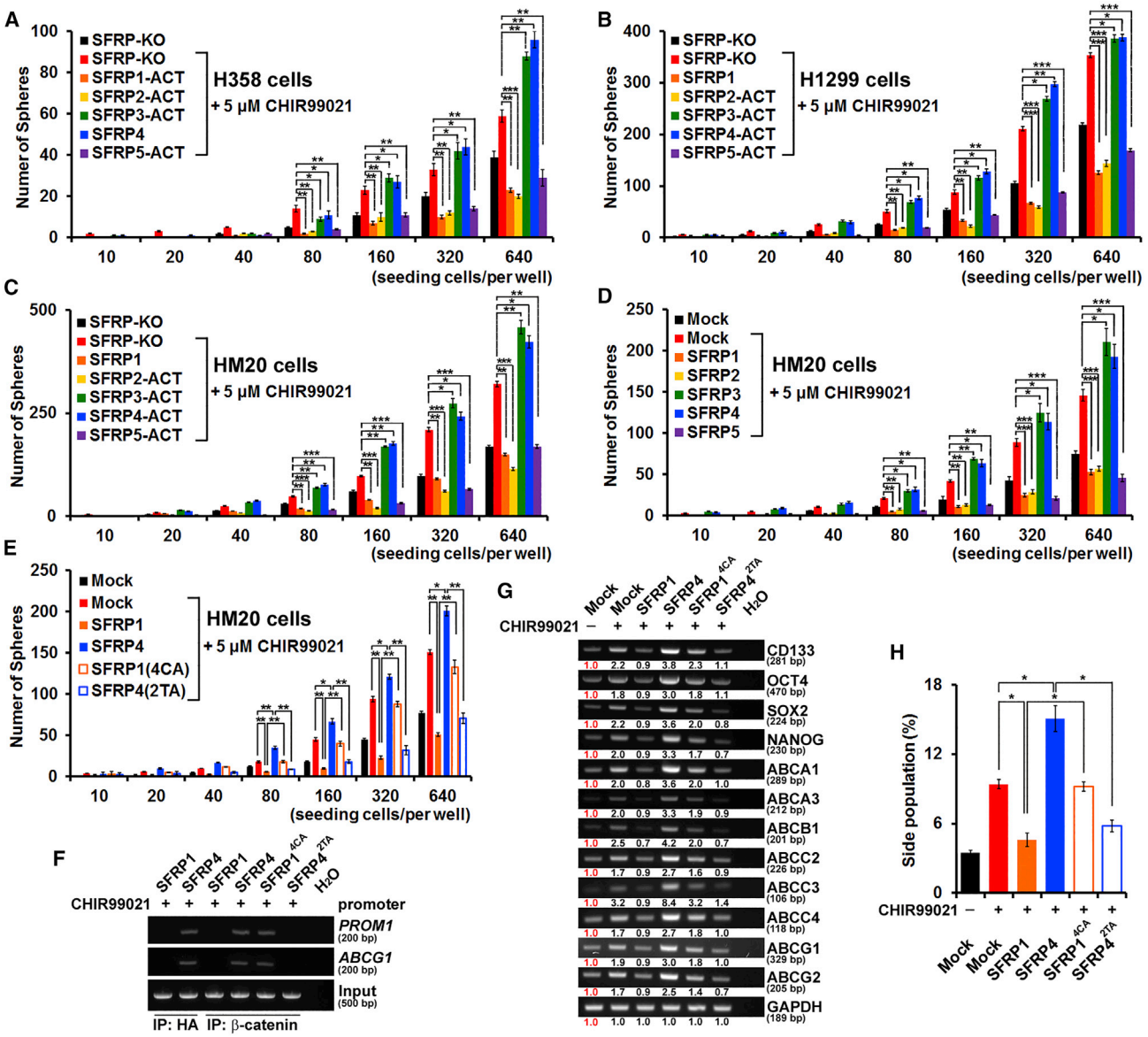

Figure 5. Nuclear SFRPs Are Potent Modulators of Wnt/β-catenin-Elicited Promotion of the CSC Phenotype

(A–C) A limiting dilution assay was performed on SFRP-expressing modified cells (H358 cells in A; H1299 cells in B; HM20 cells in C) by CRISPR/Cas9 technology as described in Figure 2B after treatment with 5 μM CHIR99021, and the cells were cultivated in ultra-low-attachment 96-well plates under sphere-forming conditions. The numbers of spheres were calculated using microscopic analysis after 7 days.

(D and E) A limiting dilution assay was performed on SFRP-HA-expressing (wild type in D; mutants in E) stable clones after treatment with 5 μM CHIR99021, and the cells were cultivated in ultra-low-attachment 96-well plates under sphere-forming conditions. The numbers of spheres were calculated using microscopic analysis after 7 days.

(F) Nuclear extracts were prepared from SFRP-HA-expressing (wild type and mutants) stable clones after treatment with 5 μM CHIR99021 for 24 h. For ChIP, the DNA was immunoprecipitated with anti-HA (HA-SFRP) or anti-β-catenin. Extracted DNA was analyzed by PCR using primers spanning the proximal promoter regions of *PROM1* and *ABCG1*.

(G) mRNA was prepared from SFRP-HA-expressing (wild type and mutants) stable clones after treatment with 5 μM CHIR99021 for 24 h. The expression of stem-cell-related and ABC transporter genes was evaluated by RT-PCR. The relative intensities of the bands are shown.

(H) Cells described in (F) were stained with Hoechst 33342. Side-population cells were counted.

Data in (A)–(E) and (H) were derived from three independent experiments and are presented as the mean ± SEM. *$p < 0.05$; **$p < 0.01$; ***$p < 0.005$ (t test). SFRP1^{4CA}, SFRP1(C58/68/129/133A); SFRP4^{2TA}, SFRP4(T186/189A).

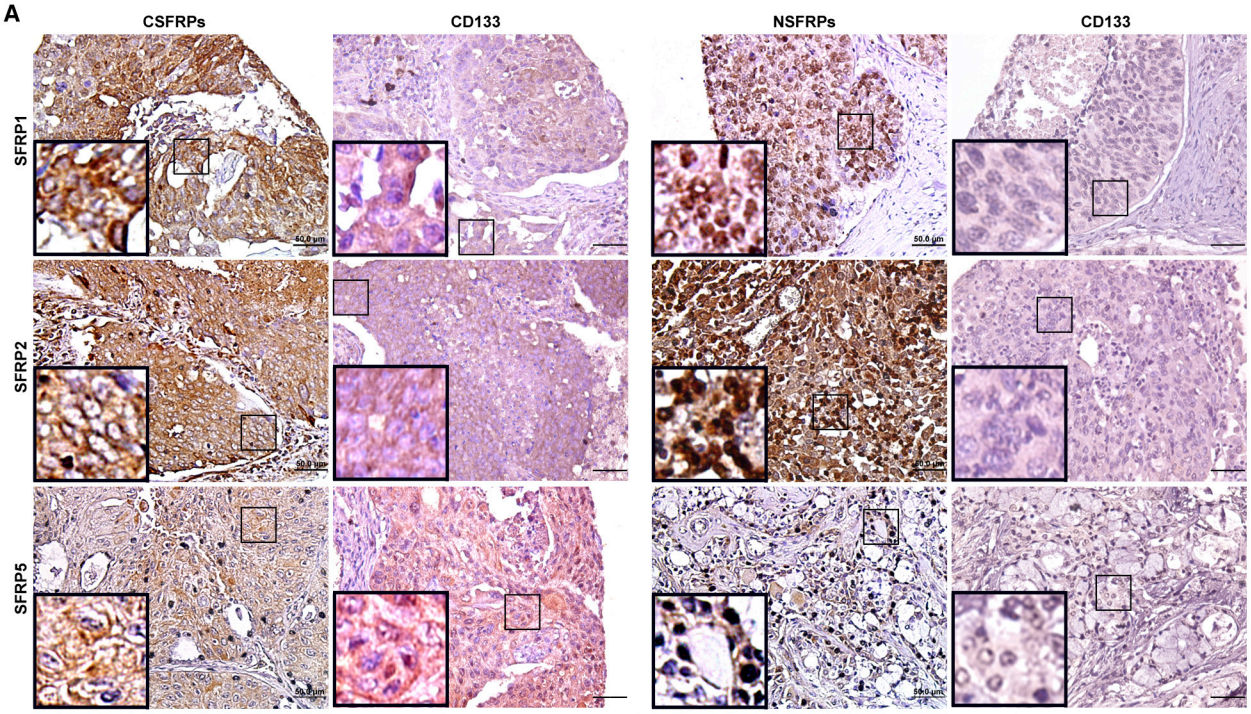

B

	SFRP1/CD133	SFRP2/CD133	SFRP3/CD133	SFRP4/CD133	SFRP5/CD133
Cytosolic SFRPs	r= 0.23/ *P*>0.1	r= -0.05/ *P*>0.5	r= 0.38/ *P*<0.02	r= 0.00/ *P*>0.5	r= 0.17/ *P*>0.2
Nuclear SFRPs	r= -0.36/ *P*<0.02	r= -0.47/ *P*<0.002	r= 0.50/ *P*<0.001	r= -0.11/ *P*>0.2	r= -0.33/ *P*<0.05

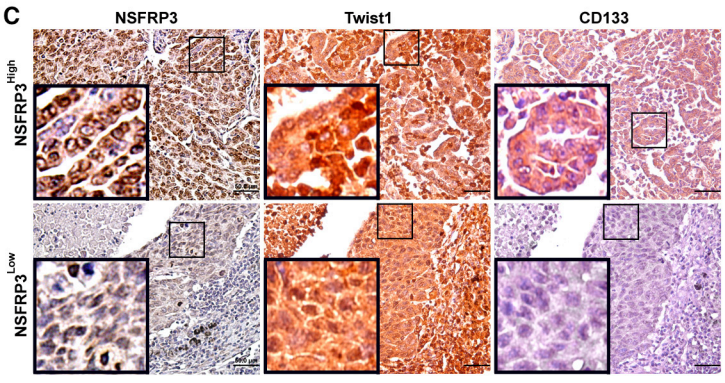

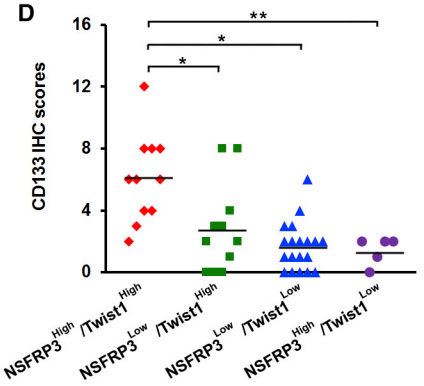

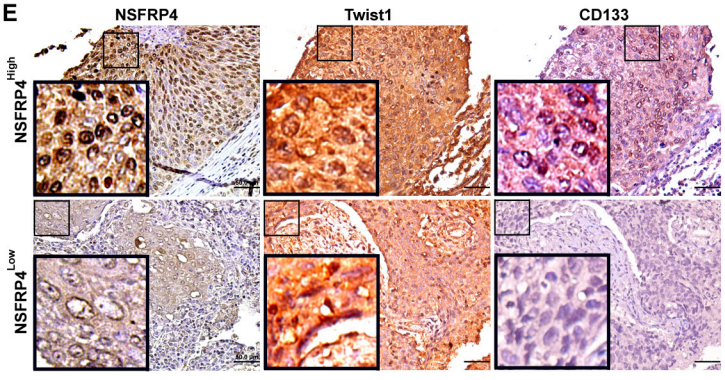

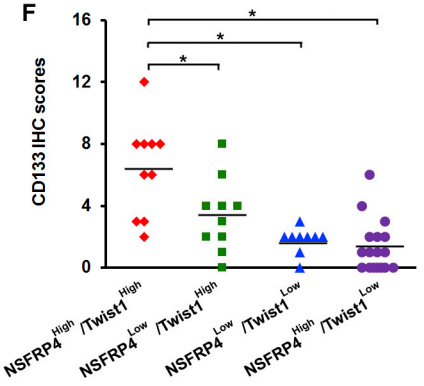

(legend on next page)

encoding sgRNAs targeting the SFRP4 promoters enhanced subcutaneous tumor growth, as compared with tumors injected with the same titer of control- sgRNA (Figure 7H). In contrast, intratumoral injections of virus particles containing constructs encoding sgRNAs targeting the SFRP1 promoters significantly suppressed subcutaneous tumor growth (Figure 7G).

Our results may provide evidence for the application of CRISPR/Cas9 targeting CSC-related genes as a treatment strategy in human cancer therapy.

DISCUSSION

As observed in previous research, SFRPs bind directly with Wnt ligands through autocrine and paracrine mechanisms (Bafico et al., 1999). However, our study suggests an alternative mechanism in which SFRPs translocate into the nucleus and bind with β-catenin. Nevertheless, the exact mechanism for the nuclear translocation of SFPRs remains unclear. Recent research shows that Wnt ligands can trigger the endocytosis of Wnt-receptor complexes and form signalosomes by binding with Frizzled and LRP6. The signalosomes recruit the destruction complex and fuse with multivesicular bodies (MVBs) (Niehrs and Acebron, 2010). SFRPs have been shown to regulate Wnt signaling by binding to Frizzled receptors (Bafico et al., 1999), and SFRPs may also rely on endocytosis by forming complexes with Wnt receptors to import themselves into the cytosol. Other observations suggest that SFRPs bind with β-catenin, which functions as a carrier involved in nuclear translocation. However, further investigation into the detailed mechanism of SFRPs nuclear translocation is needed to confirm these speculations. In this study, we show that SFRPs were secreted by exosomes (Figure 3C). We further tested if HM20 cells could naturally take up SFRP-containing exosomes. We found that extracellular SFRPs can naturally be taken up by cells by SFRPs-containing exosomes (Figures 3D and 3E). Moreover, immunofluorescence data demonstrated that SFRP1–5 co-localized with β-catenin in both the cytoplasm and nucleus (Figure 3G). The nuclear translocation of SFRPs can be abolished after knock down of β-catenin, indicating the nuclear translocation of SFRPs was β-catenin-dependent (Figure 3H).

In the canonical Wnt pathway, β-catenin serves as an important effector responsible for signal transduction. β-catenin's nuclear translocation and subsequent binding to TCF/LEF activate the transcription of Wnt target genes. The interaction between β-catenin and TCF/LEF can also be disrupted by β-catenin-interacting proteins. For example, ICAT directly interacts with β-catenin at the armadillo domain and, as a result, suppresses β-catenin/TCF4-mediated transcription (Tago et al., 2000). A nuclear protein called Chibby can also prevent TCF/LEF from interacting with β-catenin, which suppresses its transcriptional activity (Singh et al., 2007). In the interaction domain mapping experiment, we found that SFRP1–5 associated with FLAG-β-catenin-1-530 (the N terminus of β-catenin as described in Figure 4A), which included the residues Lys312 and Lys435. Moreover, SFRPs had the ability to suppress not only the interaction of TCF4 with β-catenin (Figure 3I) but also the transcriptional activity of β-catenin/TCF target genes through binding their N termini (Figure 4G). Based on these studies, we believed that nuclear SFRPs act as β-catenin-interacting proteins that regulate the Wnt signaling pathway by modulating the association between TCF4 and β-catenin.

Some data strongly indicate that SFRP4 promotes tumorigenesis through other mechanisms. As observed in colorectal carcinoma, SFRP4 was found to co-express with β-catenin, p53, and COX-2, whereas the absence of β-catenin expression was strongly associated with the loss of expression of the MLH1 mismatch repair gene. These data indicate that SFRP4 may function as an oncogene that serves as a cross-point of the Wnt and other signaling pathways (Feng Han et al., 2006). We showed that SFRP3 and SFRP4 not only enhanced the recruitment of β-catenin to TCF4 but also promoted β-catenin/TCF-mediated transcriptional activity and the CSC phenotype. Based on our findings, we suggest that SFRPs do not always function as negative modulators in the Wnt pathway. We also hypothesized that the transcriptional complex formed by β-catenin and TCF/LEF can recruit other co-activators. Consistent with our hypothesis, several studies indicate that modulators, such as nuclear Dvl and c-Jun, can bind with β-catenin and TCF4 to stabilize their interaction (Gan et al., 2008). Smad2 can also interact with β-catenin, TCF4, and

Figure 6. Clinical Significance of Nuclear SFRPs, Twist1, and CD133 in Patients with Lung Cancer

(A) Immunohistochemistry (IHC) for SFRP1, 2, and 5 and CD133 in representative tumor tissues from patients with lung cancer. Cytosolic and nuclear positivity of SFRPs in the CSFRP and NSFRP panels, respectively, was considered significant. Tissues were counterstained with hematoxylin. Left bottom, enlarged images from boxed areas as indicated. Bars, 50 mm.

(B) Results of Spearman rank tests comparing IHC scores of the various proteins among lung cancer tissues, as described in (A).

(C) IHC for SFRP3, Twist1, and CD133 in representative tumor tissues from patients with lung cancer. Using a bimodal IHC score distribution, we determined tissues with IHC scores that were lower than average were designated as having low expression, whereas scores that were higher than average were designated as having high expression. High and low nuclear positivity of SFRP3, as shown in the NSFRP3^{High} and NSFRP3^{Low} panels, respectively, was considered significant. Tissues were counterstained with hematoxylin. Left bottom, enlarged images from boxed areas as indicated. Bars, 50 mm.

(D) CD133 IHC intensity scores in the different expression patterns of NSFRP3^{High}/Twist1^{High}, NSFRP3^{Low}/Twist1^{High}, NSFRP3^{Low}/Twist1^{Low}, and NSFRP3^{High}/Twist1^{Low} in representative tumor tissues, as described in (C).

(E) IHC for SFRP4, Twist1, and CD133 in representative tumor tissues from patients with lung cancer. High and low nuclear positivity of SFRP4, as shown in the NSFRP4^{High} and NSFRP4^{Low} panels, respectively, was considered significant. Tissues were counterstained with hematoxylin. Left bottom, enlarged images from boxed areas as indicated. Bars, 50 mm.

(F) CD133 IHC intensity scores for the different expression patterns of NSFRP4^{High}/Twist1^{High}, NSFRP4^{Low}/Twist1^{High}, NSFRP4^{Low}/Twist1^{Low}, and NSFRP4^{High}/Twist1^{Low} in representative tumor tissues, as described in (E). *$p < 0.05$; **$p < 0.01$ (t test).

A

	Mock	Mock	SFRP1	SFRP2	SFRP3	SFRP4	SFRP5	SFRP1(4CA)	SFRP4(2TA)
CHIR99021 (5 uM)	-	+	+	+	+	+	+	+	+
Tumorigenesis (10^2 cells)	1/5	3/5	0/5	0/5	5/5	5/5	0/5	3/5	2/5

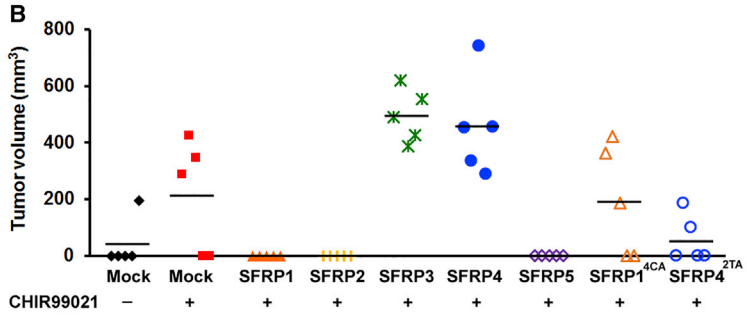

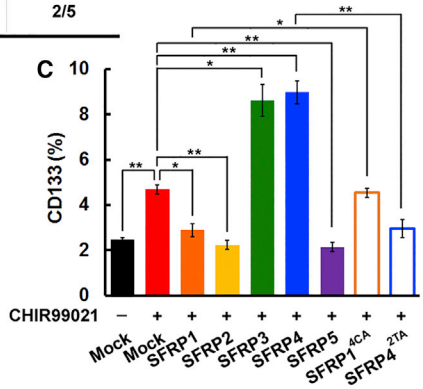

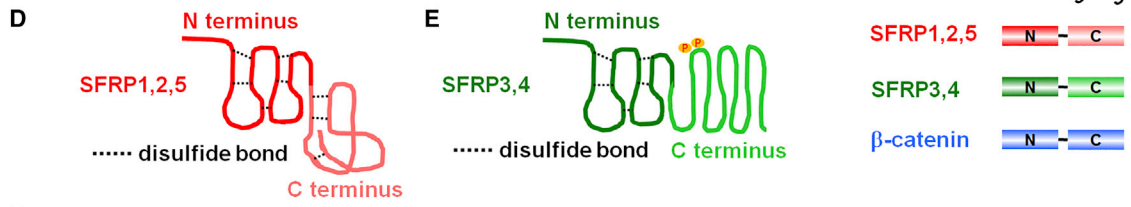

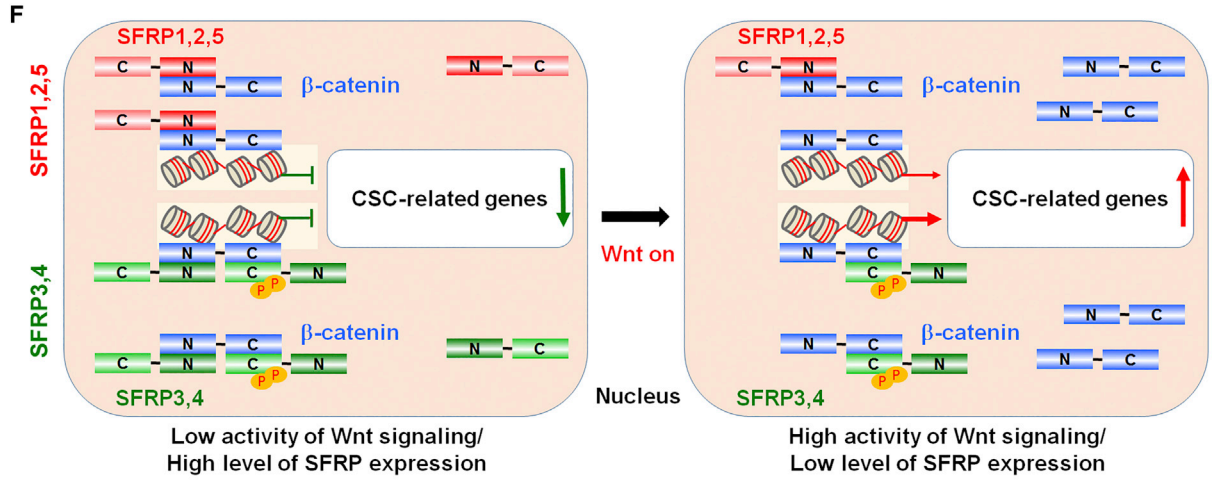

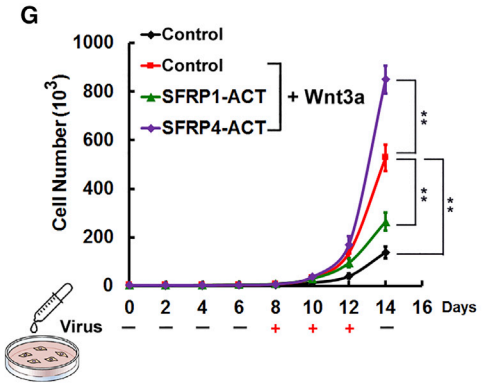

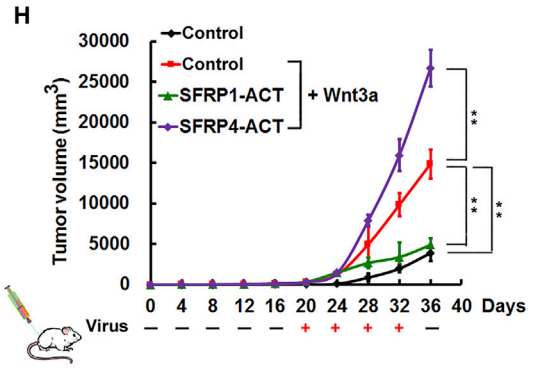

(legend on next page)

p300 to facilitate the transcriptional activity of the Wnt signaling pathway (Hirota et al., 2008). In our study, we found that SFRP3 and SFRP4 upregulated the Wnt signaling pathway. We believe that SFRP3 may be involved in recruiting unknown enhancers to activate the Wnt pathway. However, the detailed mechanism for how SFRP3 and SFRP4 regulate Wnt signaling by associating with β-catenin remains an interesting subject to be elucidated in further studies.

It has been demonstrated that SFRP1 and SFRP2 can directly bind Wnt3a and specifically block Wnt3a activity (Wawrzak et al., 2007). Indeed, the SFRP family is widely accepted as a critical Wnt modulator that blocks upstream Wnt signaling through extracellular control. However, our results showed that after SFRP treatment, the Wnt signaling pathway was also modulated in cells treated with CHIR99021 (Li et al., 2013), a GSK3β-specific inhibitor that activates the Wnt signaling pathway by bypassing extracellular control. We were surprised to find that SFRPs could regulate the Wnt signaling pathway beyond extracellular modulation. In particular, SFRPs could regulate the β-catenin/TCF transcriptional activity without interacting with Wnt3a extracellularly. Therefore, we conclude that the regulation of the Wnt signaling pathway by SFRPs is achieved by the intracellular modulation of SFRPs, as well as their extracellular functions.

In our study, SFRPs regulated the Wnt signaling pathway by associating with β-catenin in the nucleus. SFRP1, SFRP2, and SFRP5 bound with β-catenin and repressed the interaction of β-catenin and TCF4, whereas SFRP3 and SFRP4 facilitated the association of β-catenin with TCF4. This intracellular regulation of SFRPs modulates not only the transcriptional activity of the Wnt signaling pathway but also the CSC characteristics of cancer cells. In summary, our findings provide a framework for an alternative mechanism detailing the effect of SFRPs on the Wnt signaling pathway that links CSC phenotypes in human cancers.

STAR★METHODS

Detailed methods are provided in the online version of this paper and include the following:

- KEY RESOURCES TABLE
- LEAD CONTACT AND MATERIALS AVAILABILITY
- EXPERIMENTAL MODEL AND SUBJECT DETAILS
  - Human Samples
  - Animals
  - Cell Lines
- METHOD DETAILS
  - Plasmid Constructs
  - Immunohistochemistry Analysis
  - CRISPR/Cas9 Genome and Epigenome Editing
  - Cellular Fractionation
  - Exosome Purification
  - Western Blotting (WB)
  - Sphere-Forming Culture
  - Identification of Side Population (SP) cells
  - Chromatin Immunoprecipitation (ChIP)
  - Luciferase reporter assay
  - Microarray Data Collection and Analysis
- QUANTIFICATION AND STATISTICAL ANALYSIS
- DATA AND CODE AVAILABILITY

SUPPLEMENTAL INFORMATION

Supplemental Information can be found online at https://doi.org/10.1016/j.celrep.2019.07.023.

Figure 7. CRISPR/Cas9-Mediated Genome and Epigenome Editing for Precision Modulation of SFRP Expression to Control Tumor Growth *In Vivo*

(A and B) For *in vivo* tumorigenicity assays, mice (n = 5 mice per group described in A) were injected subcutaneously with 10^2 cells (SFRP-HA-expressing stable clones and mutants) in 100 mL of a 1:1 mixture of DMEM (with or without 5 μM CHIR99021)/Matrigel. Mice were euthanized at 28 days after transplantation. Tumor volumes were evaluated at 28 days after transplantation and shown in (B).

(C) Cancer cells (n = 5 cells from 5 mice per group) derived from the xenografts described in (A) were analyzed. The level of CD133 expression was determined by flow cytometry.

(D and E) Schematic models of SFRP1, 2, and 5 (D) and SFRP3-4 (E). Experimentally determined disulfide structures (solid lines connecting cysteines) and cysteine spacings of SFRPs are shown. P, two threonine phosphorylation events of SFRP3-4.

(F) In the cell nucleus, the N terminus of SFRP1–5 (disulfide bonds are required) forms a complex with the N terminus of β-catenin and acts as a negative regulator of Wnt-signaling-elicited reprogramming of the CSC phenotype, whereas the C terminus of SFRP3-4 (two threonine phosphorylation events are required) forms a complex with the C terminus of β-catenin and acts as a positive regulator of Wnt signaling. The binding affinity between the C termini of SFRP3-4 and β-catenin is higher than that between the N termini of these proteins. However, Wnt signaling is inhibited when both the N and C terminus of β-catenin bind to SFRP3-4, emphasizing that the effect of SFRPs on modulating Wnt signaling is more significant for N terminus binding. Taken together, our results show that SFRP3-4 exert a biphasic effect on Wnt activity by reducing β-catenin transcriptional activity at high concentrations (by low Wnt activity; left panel) but increasing this activity at lower concentrations (by high Wnt activity; right panel).

(G) dCas9-P300 stable clones (1,000/ml) with or without Wnt3a treatment were cultured under sphere-forming conditions. After 8 days, these spheres reached an approximate average volume (spheres with a diameter > 30 μm) and would be infected every other day for a period of 5 days with specific viral particles containing constructs encoding sgRNAs that were designed to target the SFRP1 and SFRP4 promoters. For each control and experimental condition, the same titer of viral particles was used. Total viable cell number was determined every other day for a period of 14 days.

(H) For *in vivo* tumor growth assays, mice were injected subcutaneously with 10^2 cells (dCas9-P300 stable clones) in 100 mL of a 1:1 mixture of DMEM (with or without Wnt3a)/Matrigel. After 20 days, these tumors reached an approximate average volume and would be injected intratumorally every 4 days for a period of 13 days with specific viral particles containing constructs encoding sgRNAs that were designed to target the SFRP1 and SFRP4 promoters. For each control and experimental condition, the same titer of viral particles was used. Mice were euthanized at 36 days after transplantation. Tumor volumes were evaluated every 4 days for a period of 36 days after transplantation.

Data were derived from three independent experiments and are presented as the mean ± SEM. *$p < 0.05$; **$p < 0.01$ (t test).

ACKNOWLEDGMENTS

We acknowledge access to the Biomedical Science and Engineering Center, National Tsing Hua University, Hsinchu, Taiwan and Wen-Ching Wang for technical advice regarding the use of the FACSAria III (BD Biosciences) flow cytometer. This work was supported by funds from the Taiwan Ministry of Science and Technology (grant 105-2320-B-007-004-MY3).

AUTHOR CONTRIBUTIONS

Designed, performed and analyzed the experiments, C.-J.L., Z.-W.W., and Y.-W.C.; assisted in the interpretation of the results, K.-C.L. and W.-H.L.; wrote and edited the paper, C.-J.L., Z.-W.W., K.-C.L., and J.-L.L.

DECLARATION OF INTERESTS

The authors declare no competing interests.

Received: July 19, 2017
Revised: May 31, 2019
Accepted: July 9, 2019
Published: August 6, 2019

REFERENCES

Bafico, A., Gazit, A., Pramila, T., Finch, P.W., Yaniv, A., and Aaronson, S.A. (1999). Interaction of frizzled related protein (FRP) with Wnt ligands and the frizzled receptor suggests alternative mechanisms for FRP inhibition of Wnt signaling. J. Biol. Chem. *274*, 16180–16187.

Bisson, I., and Prowse, D.M. (2009). WNT signaling regulates self-renewal and differentiation of prostate cancer cells with stem cell characteristics. Cell Res. *19*, 683–697.

Chang, Y.W., Su, Y.J., Hsiao, M., Wei, K.C., Lin, W.H., Liang, C.L., Chen, S.C., and Lee, J.L. (2015). Diverse Targets of β-Catenin during the Epithelial-Mesenchymal Transition Define Cancer Stem Cells and Predict Disease Relapse. Cancer Res. *75*, 3398–3410.

Cheng, Y.Y., Yu, J., Wong, Y.P., Man, E.P., To, K.F., Jin, V.X., Li, J., Tao, Q., Sung, J.J., Chan, F.K., and Leung, W.K. (2007). Frequent epigenetic inactivation of secreted frizzled-related protein 2 (SFRP2) by promoter methylation in human gastric cancer. Br. J. Cancer *97*, 895–901.

Chong, J.M., Uren, A., Rubin, J.S., and Speicher, D.W. (2002). Disulfide bond assignments of secreted Frizzled-related protein-1 provide insights about Frizzled homology and netrin modules. J. Biol. Chem. *277*, 5134–5144.

Chung, M.T., Lai, H.C., Sytwu, H.K., Yan, M.D., Shih, Y.L., Chang, C.C., Yu, M.H., Liu, H.S., Chu, D.W., and Lin, Y.W. (2009). SFRP1 and SFRP2 suppress the transformation and invasion abilities of cervical cancer cells through Wnt signal pathway. Gynecol. Oncol. *112*, 646–653.

Ehtesham, M., Kabos, P., Gutierrez, M.A., Chung, N.H., Griffith, T.S., Black, K.L., and Yu, J.S. (2002a). Induction of glioblastoma apoptosis using neural stem cell-mediated delivery of tumor necrosis factor-related apoptosis-inducing ligand. Cancer Res. *62*, 7170–7174.

Ehtesham, M., Kabos, P., Kabosova, A., Neuman, T., Black, K.L., and Yu, J.S. (2002b). The use of interleukin 12-secreting neural stem cells for the treatment of intracranial glioma. Cancer Res. *62*, 5657–5663.

Feng Han, Q., Zhao, W., Bentel, J., Shearwood, A.M., Zeps, N., Joseph, D., Iacopetta, B., and Dharmarajan, A. (2006). Expression of sFRP-4 and beta-catenin in human colorectal carcinoma. Cancer Lett. *231*, 129–137.

Gan, X.Q., Wang, J.Y., Xi, Y., Wu, Z.L., Li, Y.P., and Li, L. (2008). Nuclear Dvl, c-Jun, beta-catenin, and TCF form a complex leading to stabilization of beta-catenin-TCF interaction. J. Cell Biol. *180*, 1087–1100.

He, B., Lee, A.Y., Dadfarmay, S., You, L., Xu, Z., Reguart, N., Mazieres, J., Mikami, I., McCormick, F., and Jablons, D.M. (2005). Secreted frizzled-related protein 4 is silenced by hypermethylation and induces apoptosis in beta-catenin-deficient human mesothelioma cells. Cancer Res. *65*, 743–748.

Hirota, M., Watanabe, K., Hamada, S., Sun, Y., Strizzi, L., Mancino, M., Nagaoka, T., Gonzales, M., Seno, M., Bianco, C., and Salomon, D.S. (2008). Smad2 functions as a co-activator of canonical Wnt/beta-catenin signaling pathway independent of Smad4 through histone acetyltransferase activity of p300. Cell. Signal. *20*, 1632–1641.

Lee, J.L., Wang, M.J., and Chen, J.Y. (2009). Acetylation and activation of STAT3 mediated by nuclear translocation of CD44. J. Cell Biol. *185*, 949–957.

Leimeister, C., Bach, A., and Gessler, M. (1998). Developmental expression patterns of mouse sFRP genes encoding members of the secreted frizzled related protein family. Mech. Dev. *75*, 29–42.

Li, C., Zhang, S., Lu, Y., Zhang, Y., Wang, E., and Cui, Z. (2013). The roles of Notch3 on the cell proliferation and apoptosis induced by CHIR99021 in NSCLC cell lines: a functional link between Wnt and Notch signaling pathways. PLoS One *8*, e84659.

Lin, K., Wang, S., Julius, M.A., Kitajewski, J., Moos, M., Jr., and Luyten, F.P. (1997). The cysteine-rich frizzled domain of Frzb-1 is required and sufficient for modulation of Wnt signaling. Proc. Natl. Acad. Sci. USA *94*, 11196–11200.

Lin, Y.W., Shih, Y.L., Lien, G.S., Suk, F.M., Hsieh, C.B., and Yan, M.D. (2014). Promoter methylation of SFRP3 is frequent in hepatocellular carcinoma. Dis. Markers *2014*, 351863.

Mani, S.A., Guo, W., Liao, M.J., Eaton, E.N., Ayyanan, A., Zhou, A.Y., Brooks, M., Reinhard, F., Zhang, C.C., Shipitsin, M., et al. (2008). The epithelial-mesenchymal transition generates cells with properties of stem cells. Cell *133*, 704–715.

Niehrs, C., and Acebron, S.P. (2010). Wnt signaling: multivesicular bodies hold GSK3 captive. Cell *143*, 1044–1046.

Reya, T., and Clevers, H. (2005). Wnt signalling in stem cells and cancer. Nature *434*, 843–850.

Scardigli, R., Gargioli, C., Tosoni, D., Borello, U., Sampaolesi, M., Sciorati, C., Cannata, S., Clementi, E., Brunelli, S., and Cossu, G. (2008). Binding of sFRP-3 to EGF in the extra-cellular space affects proliferation, differentiation and morphogenetic events regulated by the two molecules. PLoS One *3*, e2471.

Shiota, M., Izumi, H., Tanimoto, A., Takahashi, M., Miyamoto, N., Kashiwagi, E., Kidani, A., Hirano, G., Masubuchi, D., Fukunaka, Y., et al. (2009). Programmed cell death protein 4 down-regulates Y-box binding protein-1 expression via a direct interaction with Twist1 to suppress cancer cell growth. Cancer Res. *69*, 3148–3156.

Singh, A.M., Li, F.Q., Hamazaki, T., Kasahara, H., Takemaru, K., and Terada, N. (2007). Chibby, an antagonist of the Wnt/beta-catenin pathway, facilitates cardiomyocyte differentiation of murine embryonic stem cells. Circulation *115*, 617–626.

Su, Y.J., Lai, H.M., Chang, Y.W., Chen, G.Y., and Lee, J.L. (2011). Direct reprogramming of stem cell properties in colon cancer cells by CD44. EMBO J. *30*, 3186–3199.

Su, Y.J., Chang, Y.W., Lin, W.H., Liang, C.L., and Lee, J.L. (2015a). An aberrant nuclear localization of E-cadherin is a potent inhibitor of Wnt/β-catenin-elicited promotion of the cancer stem cell phenotype. Oncogenesis *4*, e157.

Su, Y.J., Lin, W.H., Chang, Y.W., Wei, K.C., Liang, C.L., Chen, S.C., and Lee, J.L. (2015b). Polarized cell migration induces cancer type-specific CD133/integrin/Src/Akt/GSK3β/β-catenin signaling required for maintenance of cancer stem cell properties. Oncotarget *6*, 38029–38045.

Tago, K., Nakamura, T., Nishita, M., Hyodo, J., Nagai, S., Murata, Y., Adachi, S., Ohwada, S., Morishita, Y., Shibuya, H., and Akiyama, T. (2000). Inhibition of Wnt signaling by ICAT, a novel beta-catenin-interacting protein. Genes Dev. *14*, 1741–1749.

Terry, K., Magan, H., Baranski, M., and Burrus, L.W. (2000). Sfrp-1 and sfrp-2 are expressed in overlapping and distinct domains during chick development. Mech. Dev. *97*, 177–182.

Tsai, Y.P., Yang, M.H., Huang, C.H., Chang, S.Y., Chen, P.M., Liu, C.J., Teng, S.C., and Wu, K.J. (2009). Interaction between HSP60 and beta-catenin promotes metastasis. Carcinogenesis *30*, 1049–1057.

Uren, A., Reichsman, F., Anest, V., Taylor, W.G., Muraiso, K., Bottaro, D.P., Cumberledge, S., and Rubin, J.S. (2000). Secreted frizzled-related protein-1 binds directly to Wingless and is a biphasic modulator of Wnt signaling. J. Biol. Chem. *275*, 4374–4382.

Veeck, J., Geisler, C., Noetzel, E., Alkaya, S., Hartmann, A., Knüchel, R., and Dahl, E. (2008). Epigenetic inactivation of the secreted frizzled-related protein-5 (SFRP5) gene in human breast cancer is associated with unfavorable prognosis. Carcinogenesis *29*, 991–998.

Wawrzak, D., Métioui, M., Willems, E., Hendrickx, M., de Genst, E., and Leyns, L. (2007). Wnt3a binds to several sFRPs in the nanomolar range. Biochem. Biophys. Res. Commun. *357*, 1119–1123.

STAR★METHODS

KEY RESOURCES TABLE

REAGENT or RESOURCE	SOURCE	IDENTIFIER
Antibodies		
Rabbit polyclonal anti-SFRP1	Abcam	Cat#ab4193; RRID: AB_304357
Rabbit polyclonal anti-SFRP2	Santa Cruz	Cat#sc-13940; RRID: AB_2187087
Goat polyclonal anti-SFRP3	Santa Cruz	Cat#sc-7427; RRID: AB_641278
Goat polyclonal anti-SFRP4	Abnova	Cat#PAB15663; RRID: AB_10677229
Rabbit polyclonal anti-SFRP5	Thermo Fisher	Cat#PA5-71770; RRID: AB_2717624
Rabbit monoclonal anti-Wnt3a	Cell Signaling	Cat#2721; RRID: AB_2215411
Mouse monoclonal anti-HA	BioLegend	Cat#901503; RRID: AB_2565005
Rabbit polyclonal anti-PS1490-LRP6	Cell Signaling	Cat#2568; RRID: AB_2139327
Rabbit polyclonal anti-PT1479-LRP6	Abnova	Cat#PAB12632; RRID: AB_10554131
Rabbit monoclonal anti-LRP6	Cell Signaling	Cat#2560; RRID: AB_2139329
Rabbit polyclonal anti-PS9-GSK3β	Cell Signaling	Cat#9336; RRID: AB_331405
Rabbit monoclonal anti-GSK3β	Cell Signaling	Cat#9315; RRID: AB_490890
Rabbit polyclonal anti-β-catenin	Sigma	Cat#C2206; RRID: AB_476831
Rabbit polyclonal anti-Tubulin 4a	GeneTex	Cat#GTX112141; RRID: AB_10728390
Rabbit polyclonal anti-Lamin A/C	GeneTex	Cat#GTX101126; RRID: AB_10617300
Mouse monoclonal anti-CD81	Santa Cruz	Cat#sc-166029; RRID: AB_2275892
Mouse monoclonal anti-TCF4	Sigma	Cat#T5817; RRID: AB_261713
Rabbit polyclonal anti-Twist1	Thermo Fisher	Cat#PA5-49688; RRID: AB_2635141
Rabbit polyclonal anti-CD133	Abcam	Cat#ab19898; RRID: AB_470302
Biological Samples		
Human lung cancer specimens	Super Bio Chips	Cat#CCA4
Chemicals, Peptides, and Recombinant Proteins		
B-27 Supplement	Invitrogen	Cat#17504044
EGF	Prospec	Cat# CYT-217A
FGF-2	Prospec	Cat# CYT-218B
CHIR99021	Sigma	Cat#SML1046
Critical Commercial Assays		
Dual-Luciferase Reporter assay	Promega	Cat#RE1960
SS Polymer-HRP detection Kit / DAB	Biogenex	Cat#QD400
Experimental Models: Cell Lines		
Human: HM20 cells	Chang et al., 2015	PMID: 26122848
Human: H322 cells	ATCC	CRL-5806; RRID: CVCL_1556
Human: H460 cells	ATCC	HTB-177; RRID: CVCL_0459
Human: H358 cells	ATCC	CRL-5807; RRID: CVCL_1559
Human: H1299 cells	ATCC	CRL-5803; RRID: CVCL_0060
Mouse: L cells	ATCC	CRL-2648; RRID: CVCL_4536
Mouse: L-Wnt3A cells	ATCC	CRL-2647; RRID: CVCL_0635
Experimental Models: Organisms/Strains		
Mouse: SCID CB17 female	BioLasco	N/A
Oligonucleotides		
Primers for reverse transcription PCR, see Table S1	This paper	N/A
SFRP1 Knockout CRISPR SgRNA: GGCGCGGCGCTT CTGGCCGT	National RNAi Core Facility, Academia Sinica	N/A

(*Continued on next page*)

Continued

REAGENT or RESOURCE	SOURCE	IDENTIFIER
SFRP4 Knockout CRISPR SgRNA: GCAGCGCCA CTAGGATGGAG	National RNAi Core Facility, Academia Sinica	N/A
SFRP1 Activation CRISPR SgRNA: TAAACCGAAC CCGCTCGCGA	National RNAi Core Facility, Academia Sinica	N/A
SFRP2 Activation CRISPR SgRNA: CCCTTCCAGC AAGCGCGTGA	National RNAi Core Facility, Academia Sinica	N/A
SFRP3 Activation CRISPR SgRNA: TTGTGTGCG TGATCTAGGGG	National RNAi Core Facility, Academia Sinica	N/A
SFRP4 Activation CRISPR SgRNA: TTTCGACACC GGATACAAGA	National RNAi Core Facility, Academia Sinica	N/A
SFRP5 Activation CRISPR SgRNA: CTGGGCGGG ACGCTCGGGCA	National RNAi Core Facility, Academia Sinica	N/A
siRNA targeting YKT6	Sigma	CAT# NM_006555
siRNA targeting β-catenin	Cell Signaling	CAT#6238
Recombinant DNA		
pReceiver-M45-SFRP1	This paper	N/A
pReceiver-M45-SFRP2	This paper	N/A
pReceiver-M45-SFRP3	This paper	N/A
pReceiver-M45-SFRP4	GeneCopoeia	Cat#EX-Q0456-M45
pReceiver-M45-SFRP5	This paper	N/A
pReceiver-M45-SFRP1/N	This paper	N/A
pReceiver-M45-SFRP1/C	This paper	N/A
pReceiver-M45-SFRP2/N	This paper	N/A
pReceiver-M45-SFRP2/C	This paper	N/A
pReceiver-M45-SFRP3/N	This paper	N/A
pReceiver-M45-SFRP3/C	This paper	N/A
pReceiver-M45-SFRP4/N	This paper	N/A
pReceiver-M45-SFRP4/C	This paper	N/A
pReceiver-M45-SFRP5/N	This paper	N/A
pReceiver-M45-SFRP5/C	This paper	N/A
pReceiver-M45-SFRP1(4CA)	This paper	N/A
pReceiver-M45-SFRP4(2TA)	This paper	N/A
pReceiver-M45-Twist1	This paper	N/A
pFlag-β-catenin	Tsai et al., 2009	PMID: 19369584
pFlag-β-catenin-1-530	Tsai et al., 2009	PMID: 19369584
pFlag-β-catenin-531-827	Tsai et al., 2009	PMID: 19369584
M50 Super 8x TOPFlash	Addgene	Cat#12456
M51 Super 8x FOPFlash	Addgene	Cat#12457
Software and Algorithms		
ImageJ		https://imagej.nih.gov/ij/

LEAD CONTACT AND MATERIALS AVAILABILITY

This study did not generate new unique reagents. Further information and requests for resources and reagents may be directed to and will be fulfilled by Lead Contact, Dr. Jia-Lin Lee (jllee@life.nthu.edu.tw).

EXPERIMENTAL MODEL AND SUBJECT DETAILS

Human Samples

Sectioned human lung cancer specimens were obtained from Super Bio Chips (Cat#CCA4). Please see Table S2 for details on clinical information of human tissue samples.

Animals

Severe combined immunodeficient (SCID) CB17 female mice (6 weeks old) were used, and all experimental protocols were approved by the Institutional Animal Care and Use Committee (IACUC) at National Tsing Hua University, Hsinchu 30013, Taiwan. For the *in vivo* tumorigenicity assay, mice were injected subcutaneously with 10^2 cells in 100 μL of a mixture of DMEM (with or without Wnt3a)/Matrigel (1:1). Tumorigenicity was evaluated at 4 weeks after transplantation. For *in vivo* SFRPs-expressing modified by CRISPR/Cas9 technology, mice were injected subcutaneously with 10^2 cells (dCas9-P300 stable clones) in 100 mL of a 1:1 mixture of DMEM (with or without Wnt3a)/Matrigel. After 20 days, these tumors reached an approximate average volume, and would be injected intratumorally every 4 days for a period of 13 days with specific viral particles containing constructs encoding sgRNAs were designed to target the SFRP1 and SFRP4 promoters. For each control and experimental condition, the same titer of viral particles was used. Mice were euthanized at 36 days after transplantation. Tumor volumes were evaluated every 4 days for a period of 36 days after transplantation.

Cell Lines

Human lung cancer H322 cells (ATCC, CRL-5806), H358 cells (ATCC, CRL-5807), H460 cells (ATCC, HTB-177) and H1299 cells (ATCC, CRL-5803) were cultured under standard conditions in RPMI-1640 (Invitrogen) supplemented with 10% FBS (Biological Industries) and 1% Penicillin/Sreptomycin/ Amphotericin B (Biological Industries) and incubated in 5% humidified CO2 incubator at 37°C. Mouse fibroblast L cells (ATCC, CRL-2648) and L Wnt-3A cells (ATCC, CRL-2647) were cultured under standard conditions in DMEM (Invitrogen) supplemented with 10% FBS (Biological Industries) and 1% Penicillin/Sreptomycin/ Amphotericin B (Biological Industries) and incubated in 5% humidified CO2 incubator at 37°C.

Human lung cancer HM20 cells were obtained from cells fractionation by invasive assays. Through four serial passages (p4), human lung cancer A549 cell-derived spheres were transferred back to adhesive tissue culture plates, after which they migrated back onto plates and reformed a monolayer with morphological heterogeneity [and were then collected as low-motility (LM) cells] (Chang et al., 2015). To establish an EMT/metastasis cell model, LM cells were seeded onto Matrigel-coated Boyden chamber membranes. After a 24-h incubation period, the cells that had invaded the Matrigel were collected as high-motility1 (HM1) cells, signifying one passage through the basement-membrane matrix. Subsequently, these cells were regrown and passed 19 more times through the invasion-selection procedure. The cells harvested from each subsequent round of selection were designated HM2 to HM20.

METHOD DETAILS

Plasmid Constructs

The SFRP1 and SFRP2 expression constructs (Chung et al., 2009) were gifts from Ya-Wen Lin (National Defense Medical Center, Taipei, Taiwan). The SFRP3 expression construct was a gift from Giulio Cossu (Scardigli et al., 2008) (San Raffaele Biomedical Science Park of Rome, Rome, Italy). SFRP4 was purchased from GeneCopoeia, Inc. SFRP5 was purchased from Genediscovery Biotechnology. The SFRP1-5 cDNAs were amplified by PCR from the plasmids described above and subcloned into pReceiver-M45 vectors. SFRP1-5 mutants with a C-terminal deletion (SFRP1-5/N; NTR domain deleted) and an N-terminal deletion (SFRP1-5/C; CRD domain deleted) were generated by PCR amplification of the corresponding cDNA fragments using wild-type SFRP1-5 as templates (Figure 4C). The $SFRPs^{4CA}$ mutants [four cysteines (C58/68/129/133) of SFRP1, four cysteines (C40/50/114/118A) of SFRP2, four cysteines (C35/43/108/112A) of SFRP3, four cysteines (C24/32/97/101) of SFRP4 and four cysteines (C53/63/124/128A) of SFRP5 were substituted with alanine] were generated by site-directed mutagenesis using the wild-type SFRPs as templates. The $SFRP3^{2TA}$ and $SFRP4^{2TA}$ mutants [two threonine (T186/189) of SFRP3 and SFRP4 were substituted with alanine] were generated by site-directed mutagenesis using the wild-type SFRP3 and SFRP4 as templates. The correct sequence of the clones was verified by sequencing. The Twist1 expression construct (Shiota et al., 2009) was a gift from Kimitoshi Kohno (University of Occupational and Environmental Health, Kitakyushu, Japan). The Twist1 cDNAs were amplified by PCR from the plasmids described above and subcloned into pReceiver-M45 vectors. Wild-type and β-catenin mutant expression constructs with a C-terminal deletion (β-catenin/N; residues 531–781 deleted) and an N-terminal deletion (β-catenin/C; residues 1–530 deleted) were gifts from Kou-Juey Wu (Tsai et al., 2009) (China Medical University, Taichung, Taiwan). Antibodies against the following proteins were used: SFRP1 (ab4193) and CD133 (ab19898) (all from Abcam); HA epitope tag (901503; BioLegend); Lamin A/C (GTX101126) and α Tubulin 4a (GTX112141) (all from GeneTex); SFRP2 (sc-13940), SFRP3 (sc-7427) and CD81 (sc-166029) (all from Santa Cruz Biotechnology); SFRP4 (PAB15663) and PT1479-LRP6 (PAB12632) (all from Abnova); SFRP5 (PA5-71770) and Twist1 (PA5-49688) (all from Thermo Fisher); β-catenin (C2206) and TCF4 (T5817) (all from Sigma); and Wnt3a (2721), LRP6 (2560), PS1490-LRP6 (2568), LRP6 (2560), GSK3β (9315) and PS9-GSK3β (9336) (all from Cell Signaling Technology).

Immunohistochemistry Analysis

All staining procedures were performed using a Super Sensitive IHC Detection Systems kit (BioGenex). Counterstaining was performed with hematoxylin. A semiquantitative method for calculating positive signals was used. Signals were counted in six fields per sample under a light microscope at 400 × magnification. The results were manually evaluated by two independent observers to determine both the percentage of positive cells and the staining intensity, as previously described (Chang et al., 2015; Su et al., 2015a; Su et al., 2011; Su et al., 2015b). The observers were blinded to the stage of each sample. The immunohistochemistry (IHC) score was obtained by multiplying the staining intensity (0 = no expression, 1 = weak expression, 2 = moderate expression,

3 = strong expression, and 4 = very strong expression) by the percentage of positive cells (0 = 0%–5% expression, 1 = 6%–25% expression, 2 = 26%–50% expression, 3 = 51%–75% expression, and 4 = 76%–100% expression) in the field. The maximum possible IHC score was 4 × 4 = 16.

CRISPR/Cas9 Genome and Epigenome Editing

For SFRPs-knockout experiments, lentiviral vectors, pAll-Cas9.pPuro, containing the single guide RNA (sgRNA) targeting human SFRPs (SFRP1 and SFRP4) and the lentiviral vector containing the nontargeting control sgRNA, were purchased from the National RNAi Core Facility, Academia Sinica, Taipei, Taiwan. The sequences of SFRP1 and SFRP4-targeting sgRNAs were as follows: SFRP1, GGCGCGGCGCTTCTGGCCGT; SFRP4, GCAGCGCCACTAGGATGGAG. Cells were transfected with plasmids carrying the individual sgRNAs. The homozygous SFRP1 and SFRP4 knockout cells were selected by serial dilution and single-cell culturing. The knockout efficiency was confirmed by western blotting. For SFRPs-activation experiments, lentiviral vectors, pU6-Cas9.pPuro, containing the single guide RNA (sgRNA) targeting human SFRP1-5 promoters, were purchased from the National RNAi Core Facility, Academia Sinica, Taipei, Taiwan. The sequences of SFRP1-5 promoter-targeting sgRNAs were as follows: SFRP1, TAAACC GAACCCGCTCGCGA; SFRP2, CCCTTCCAGCAAGCGCGTGA; SFRP3, TTGTGTGCGTGATCTAGGGG; SFRP4, TTTCGACACCG GATACAAGA; SFRP5, CTGGGCGGGACGCTCGGGCA. Cells were transfected with plasmids carrying the individual sgRNAs. The SFRP1-5 activation cells were selected by serial dilution and single-cell culturing. The activation efficiency was confirmed by western blotting.

Cellular Fractionation

Cellular fractionation was performed as previously described (Chang et al., 2015; Lee et al., 2009; Su et al., 2015a; Su et al., 2011). Cells were lysed in lysis buffer (20 mM HEPES, pH 7.0, 10 mM KCl, 2 mM MgCl2, 0.5% Nonidet P40, 1 mM Na3VO4, 1 mM PMSF, 0.15 U/ml aprotinin) and homogenized by 30 strokes in a tightly fitting Dounce homogenizer. The homogenate was centrifuged at 1,500 g for 5 min to sediment the nuclei. The supernatant was resedimented at 15,000 g for 5 min, and the resulting supernatant formed the cytosolic fraction. The nuclear pellet was washed three times and resuspended in the same buffer containing 0.5 M NaCl to extract nuclear proteins. The extracted material was sedimented at 15,000 g for 10 min and the resulting supernatant was termed the nuclear fraction as described (Ehtesham et al., 2002b). The marker of each cellular fractionation was used to perform western blotting: Lamin A/C and Histone H3 to be nuclear markers; α-tubulin to exclude contamination of cytoplasmic fractions; Integrin β1 to exclude contamination of cytoplasmic membranes; Vti1b to exclude contamination of Golgi; EEA1 to exclude contamination of early endosome; Calnexin to exclude contamination of ER.

Exosome Purification

For exosomes secreted by cultured cell lines, conditional media (CM) was first prepared by incubating cells grown at sub-confluence in growth media containing exosome-depleted FBS (prepared by overnight ultracentrifugation at 100,000 × g at 4°C) for 48 hr, and pre-cleared by centrifugation at 500 × g for 15 min and then at 10,000 × g for 20 min. Exosomes were isolated by ultracentrifugation at 110,000 × g for 70 min, and washed in PBS using the same ultracentrifugation conditions (Ehtesham et al., 2002a).

Western Blotting (WB)

Cells were lysed using cold RIPA buffer (50 mM Tris-HCl, pH 7.5, 150 mM NaCl, 1% Triton X-100, 0.1% SDS, 1 mM DTT) supplemented with protease inhibitors (Sigma # P8340) and protein concentrations of lysate were measured by Bradford method (Bio-Rad Protein Assay #500-006). Equal amounts of proteins were separated on SDS-PAGE electrophoresis. Proteins from SDS-PAGE gel were transferred to PVDF membrane (PALL) and probed with primary and appropriate secondary antibodies. Antibodies against the following proteins were used: SFRP1 (ab4193) and CD133 (ab19898) (all from Abcam); HA epitope tag (901503; BioLegend); Lamin A/C (GTX101126) and α Tubulin 4a (GTX112141) (all from GeneTex); SFRP2 (sc-13940), SFRP3 (sc-7427) and CD81 (sc-166029) (all from Santa Cruz Biotechnology); SFRP4 (PAB15663) and PT1479-LRP6 (PAB12632) (all from Abnova); SFRP5 (PA5-71770) and Twist1 (PA5-49688) (all from Thermo Fisher); β-catenin (C2206) and TCF4 (T5817) (all from Sigma); and Wnt3a (2721), LRP6 (2560), PS1490-LRP6 (2568), LRP6 (2560), GSK3β (9315) and PS9-GSK3β (9336) (all from Cell Signaling Technology). Images were recorded using a luminescence image analyzer (FUSION SL; Vilber Lourmat) and the band intensities were quantitated by densitometry using Bio-1D and Bio-Gene software (Vilber Lourmat).

Sphere-Forming Culture

Spheres were generated as previously described (Chang et al., 2015; Su et al., 2015a; Su et al., 2011; Su et al., 2015b). Briefly, cells (1,000/ml) were grown in suspension culture using ultra-low attachment plates (Corning) and serum-free RPMI (ATCC) supplemented with B27 (Invitrogen), 20 ng/ml EGF (Prospec) and 10 ng/ml bFGF (Prospec). Spheres with a diameter > 30 μm were then counted. For serial passages, spheres were harvested and dissociated to single cells with trypsin, and then 100 dissociated cells were re-plated in a 96-well plate (an ultra-low-attachment plate) and cultured for 12 days. The spheres were then counted again. The individual spheres were found to be derived from single cells (Mani et al., 2008).

Identification of Side Population (SP) cells

SP cells were identified as previously described (Chang et al., 2015; Su et al., 2015a; Su et al., 2011; Su et al., 2015b). Briefly, cells were suspended in pre-warmed RPMI containing 2% FBS and 10 mM HEPES and stained with 5 μg/ml of Hoechst 33342 dye (Molecular Probes) for 90 min at 37°C with or without 100 μM reserpine, which is an inhibitor of some ABC transporters. Cells were then washed and resuspended in HBSS containing 2% FBS and 10 mM HEPES. Before cell sorting, 0.25 μg/ml of 7-AAD (Sigma) was added to exclude nonviable cells. The concentration of Hoechst 33342 and the incubation times were initially identified using the samples that provided the highest frequency of SP cells with the lowest cytotoxicity determined by 7-AAD staining. SP cells were analyzed on a FACSAria III (BD Biosciences) flow cytometer equipped with 424/44-nm bandpass and 670-nm longpass optical filters (Omega Optical).

Chromatin Immunoprecipitation (ChIP)

ChIP assay was performed as previously described (Chang et al., 2015; Lee et al., 2009; Su et al., 2015a; Su et al., 2011; Su et al., 2015b). Cells were fixed with1% formaldehyde for 20 min at room temperature and harvested with ChIP lysis buffer (50mM Tris pH 8.0, 85mM KCl, 1mM DTT, 1 mM PMSF, 0.5% NP-40). Genomic DNA in the lysate was sonicated using a Bioruptor (Diagenode) for 15-cycles on high power setting (30 s on, 30 s off) at 4°C. Cellular debris was removed by centrifugation at 15,000 rpm for 30 minutes at 4°C. Lysate supernatant was brought up to 1mL volume using ChIP lysis buffer and was precleared using 5 μg ssDNA and 25 μL of Protein G agarose (ThermoFisher, Cat#20399) with rotation for 1 hour at 4°C. Precleared lysates were centrifuged at 14,000 rpm for 10 minutes and lysate supernatant was transferred to a new tube for subsequent immunoprecipitation. 50 μL of lysate was reserved as whole-cell extract input control. Anti-HA was used for immunoprecipitation. Antibody was recovered using Protein G agarose (ThermoFisher). Immunoprecipitated DNA or input DNA was analyzed by PCR using primers spanning the proximal (nucleotide positions −351/-152) promoter regions of *PROM1* or (−382/-183) promoter regions of *ABCG1*. Following 30 cycles of amplification, PCR products were run on a 1.5% agarose gel and analyzed by ethidium bromide staining.

Luciferase reporter assay

The luciferase reporter plasmids were purchased from Addgene (Cat#12456 and Cat#12457). The luciferase reporter plasmids were introduced into cells, as well as their respective controls. Cell lysates were harvested 24 h later and followed standard protocol of Dual-Luciferase Reporter assay (Promega, Cat#RE1960). Luciferase activities were determined and plotted as fold change of over-expressed or knockdown over the controls.

Microarray Data Collection and Analysis

Total cellular RNA was extracted from Hm20 Mock or SFRP1-5-expressing stable clones after treatment with Wnt3a-containing medium for 24 hours. The Human Whole Genome OneArray v6.2 (Phalanx Biotech, San Diego, CA) was used to perform the DNA microarray analysis.

QUANTIFICATION AND STATISTICAL ANALYSIS

Data are represented as mean ± SEM, and experiments were performed at least in triplicate. Differences between two groups were examined by Student's t test. The Spearman correlation coefficient was used to assess the association between two continuous variables. Differences were statistically significant at $p < 0.05$.

DATA AND CODE AVAILABILITY

The accession number for the microarray data reported in this paper is GEO: GSE133943 and is accessible through the NCBI's Gene Expression Omnibus (GEO).